IEEE Access
Multidisciplinary | Rapid Review | Open Access Journal

Received 17 May 2022, accepted 19 June 2022, date of publication 23 June 2022, date of current version 21 July 2022.

Digital Object Identifier 10.1109/ACCESS.2022.3185662

Improved Instantaneous Reactive Power (PQ) Theory Based Control of DVR for Compensating Extreme Sag and Swell

SAAD F. AL-GAHTANI[1], ELBARBARY Z. M. SALEM[1,2], SHAIK M. IRSHAD[1], AND HAITHAM ZAKI AZAZI[3]

[1]Electrical Engineering Department, College of Engineering, King Khalid University, Abha 61411, Saudi Arabia
[2]Department of Electrical Engineering, Faculty of Engineering, Kafrelsheikh University, Kafrelsheikh 33516, Egypt
[3]Electrical Engineering Department, Faculty of Engineering, Menoufia University, Shebin El-kom 32511, Egypt

Corresponding author: Haitham Zaki Azazi (haitham_azazi@yahoo.com)

This work was supported by the Deanship of Scientific Research through the King Khalid University under Grant RGP.1/223/43.

ABSTRACT In today's power system, power quality is a critical topic having several impacts on customers and utilities. In the current electric power system, the integration of renewable energy sources, smart grid technologies, and significant usage of power electronics equipment has generated a slew of issues. The sensitive equipment might be damaged by harmonics, voltage sag, and swell. These devices are vulnerable to Interference with other elements of the system resulting in input voltage changes. As a result, in the contemporary period, Power quality is becoming more important as the number of sensitive and costly electronic devices grows. To overcome the challenges of non-standard voltage, the Dynamic Voltage restorer (DVR) device has been extensively utilized to keep the load voltage stable. To have a dynamic and fast response of the DVR a modified instantaneous reactive power (PQ) theory is proposed to control DVR under extreme transient voltage circumstances. The proposed technique is based on the extraction of the positive sequence component of grid voltage and the negative sequence component of load current for generating a voltage reference signal. The power system network with the proposed PQ control scheme is investigated and assessed under various scenarios to compensate for severe balanced, unbalanced (voltage sags and swells), and load change. MATLAB/Simulink is used to verify the mathematical models of the conventional PQ and proposed PQ control system for DVR. The complete system is implemented experimentally using a dSPACE 1104 based laboratory system to validate the presented control scheme. The simulation and experimental results are correlated, demonstrating the efficacy of the suggested modified PQ control technique.

INDEX TERMS Instantaneous reactive power (PQ) theory, dynamic voltage restorer (DVR), balanced and unbalanced load, voltage sag, voltage swell, load change.

I. INTRODUCTION

Power quality is a criterion of a pure and regularized power supply in terms of load. Many factors, including sensitive, non-linear loads, the integration of distributed generation (DG), and advancements in power electronics equipment affect the power quality of the grid [1], [2]. Electrical power quality has massive consideration in the electrical distribution system. The major source of concern is power quality issues relating to distribution system voltage stability [3]. Voltage sag and swell are the two most common power quality issues that impact sensitive loads [4]. Voltage sag is defined as an abrupt fall in the amplitude of supply voltage to a level of 10-90% [5], [6]. Short circuit faults in power systems lead to voltage sags. Many disadvantages have been explored in recent years resulting from voltage sags, such as electrical equipment malfunctioning, loss in the manufacturing line, and complete equipment failure [7], [8]. Voltage swell is defined as the rise in voltage level to 110-180% of its rated value. Voltage swell is the result of sudden disconnection

The associate editor coordinating the review of this manuscript and approving it for publication was Gayadhar Panda.

of the large load, open circuit faults. This issue will lead to insulation breakdown, overheating of electrical equipment, and damage to electronic equipment.

Essam *et al.* state that Voltage sag is a serious power quality issue that plays havoc on sensitive loads in the distribution system [9]. To compensate for power quality issues, power electronics-based devices like power filters, unified power flow controller (UPFC), static compensator (STATCOM), distribution static compensator (DSTATCOM), and dynamic voltage restorer (DVR) are used [10], [11]. DVR requires a complex control mechanism to safeguard important distribution system loads from power quality issues [12].

DVR is used on distribution feeders to safeguard loads from problems caused by voltage sags and swells. DVR is linked in series with the load, and a battery energy storage system (BESS) is coupled with a transformer and inverter, which adjust the active and reactive power requirements for voltage sags and voltage swells [13]. For voltage stability, the DVR injects voltage into the distribution system, which is connected to the system through the transformer [14]. DVR is a FACTS device that adjusts for disturbances caused by loads such as voltage sags, swells, and voltage harmonics.

In normal settings, DVR injects voltages in series with the transmission lines and injects a modest amount of voltage.

When a disturbance occurs, however, DVR calculates the voltages needed to safeguard the load using sinusoidal pulse width modulation (SPWM) [15]. The voltages are then fed back into the system to keep the condition stable. DVR either absorbs or delivers active or reactive power in the steady-state, but when a disturbance occurs, DVR either delivers or absorbs active or reactive power from the dc-link. Martiningsih *et al.* have advocated installing a DVR in a PT DSS power plant, where the DVR functions as a compensator and is linked in series with the distribution line. The suggested PI-based DVR is capable of recovering power quality constraints [16], [17]. Eltamaly *et al.* developed a DVR-based technique for reducing voltage sag using DVR to improve the quality of power systems. To deterioration in electrical equipment performance. The findings show that DVR properly compensates for sag/swell and implements suitable voltage adjustment [18]. To alleviate symmetrical and asymmetrical sags and swells, J. Han *et al.* presented a unique DVR with a power electronic transformer (PET) [19]. The findings show that the unique design efficiently alleviates the symmetrical and asymmetrical problems.

The DVR control strategy can protect the load from power quality issues related to voltage [5]. To have proper control, a perfect reference generation technique must be implemented. Various approaches for reference generation have been suggested, including, Clark's and Park's transformations, Phasor parameter and, Symmetrical components, Instantaneous real and reactive power [20].

Park's transformation is a mathematical transformation approach used to simplify the analysis of three-phase circuits is direct–quadrature–zero (dq0) in electrical engineering. The application of the dq0 transform on three-phase circuits reduces the three AC values to two DC quantities [8], [21]. The inverse transform is used to reconstruct the real three-phase AC results using simplified computations on these imaginary DC variables. It is often used to ease the study of three-phase synchronous machines as well as calculations for three-phase inverter control [22]. When applied to three-phase voltages and currents, the dq0 transform is The Phase Locked Loop (PLL) must create a signal with the same fundamental frequency and phase angle as the reference signal generation for the two approaches Clarke and Park's transformation [23].

The Phasor parameter or Phase Locked Loop (PLL) is a control system that attempts to create an output signal whose phase is allied to the phase of the input ''reference'' signal. It is an electrical circuit that consists of a phase detector and a variable frequency oscillator [24]. This circuit checks the phase of the input signal to the phase of the signal obtained from its output, then changes the frequency of its output signal to maintain the phases in synchronism [25].

The ''Generalized Theory of Instantaneous Active and Reactive Power, ''or ''Theory of Instantaneous Power,'' or simply ''PQ Theory System with a neutral wire was briefly mentioned in the original development of the theory, which was intended for three-phase, three-wire systems [7], [26], [27]. Afterward, it was expanded to three-phase four-wire systems (systems having phases a, b, and c, in addition to a neutral wire) After performing an algebraic translation (Clarke transformation) of the three-phase voltages and currents in the abc coordinates to the $\alpha\beta$ coordinates, the PQ theory instantaneous power components are calculated [6], [28], [29].

In this article, an improved PQ method is proposed for the generation of reference signals in terms of the positive sequence component of the grid voltage and the negative sequence component of load current. The appearance of load current negative sequence component arises due to power quality issues such as voltage sag, swell, load change, harmonic effect, balance, and unbalanced load [30]. The main advantage of the modified technique is the non-utilization of phase-locked loop and low-pass filters, because of which the disadvantages of phase shifting and insufficient compensation are eliminated. Comparison analysis between the performances of traditional and proposed PQ methods is presented through different scenarios of power quality issues. The proposed method is superior in detecting and compensating the power quality issues.

The paper is organized in the sections as followed. Section II provides a discussion on dynamic voltage restorer (DVR). Section III describes the proposed PQ algorithm. The experimental setup is described in Section IV. The result illustration, as well as a discussion, is presented in section V. The performance of the proposed DVR control system is summarized in Section VI.

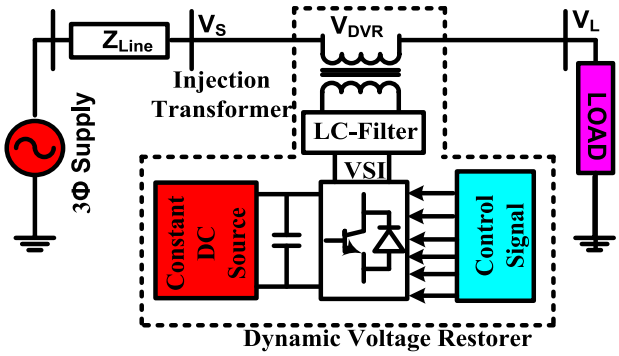

FIGURE 1. Single line diagram of power network with DVR.

II. PHILOSOPHY DYNAMIC VOLTAGE RESTORER (DVR)

Injection of compensation voltage with the precise magnitude and frequency is required to restore the load side voltage to the proper amplitude and waveform. The system may inject up to 50% of the normal voltage for a brief period of time (up to 0.1 seconds). Most voltage sags, on the other hand, are much below 50%. Dynamic voltage restoration or control is the term used to describe this (DVR) [31]. A dynamic voltage restorer (DVR) is described as the regulating device [12], [16], [32]. End-users who are experiencing power quality problems may benefit from DVRs [33]. Figure 1 depicts a simple DVR power system circuit with a control circuit to inject compensated voltage and maintain the voltage at the correct level. DVRs are often mounted on a crucial feeder, delivering active power through DC energy storage while internally generating the requisite reactive power [34], [35].

In restoring the load side voltage to the required level, a compensating voltage of the required magnitude and frequency must be injected [36]–[39]. The system can inject up to 50% of the rated voltage, but only for a brief period (up to 0.1 seconds). Normally voltage sags, are far smaller than 50%. A dynamic voltage restorer (DVR) is the regulating device. DVRs may be useful for end-users who are prone to undesirable power quality issues [40]. DVRs are often mounted on the main feeder, delivering active power through DC energy storage and generating the requisite reactive power internally [30], [41].

A. DVR OPERATING MODES

A DVR's switching states are classified into three categories based on operating states: protective, standby, and voltage compensation [42]. In the protective state, if the load current exceeds the allowable value owing to a short circuit or a significant overcurrent current, the DVR will be disconnected from the grid [43]. The inverter shorts the secondary winding of the injection transformer. In the standby state, allowing full load current to flow through the primary winding. In this operation mode, the DVR will not inject any correction voltage into the power grid. In the voltage compensation state,

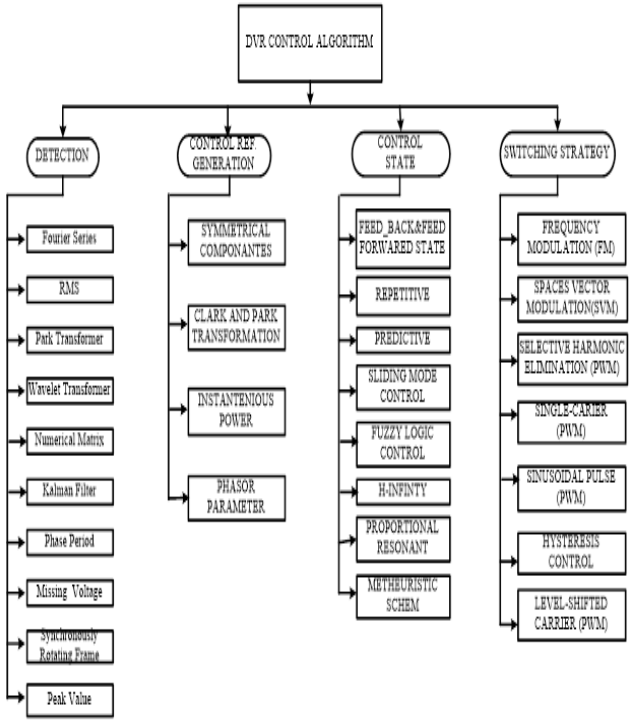

FIGURE 2. Flow chart for control strategies of DVR.

the DVR injects the appropriate compensatory voltage via injection transformer to the grid [44]. This mode of operation begins when a load voltage disturbance is detected and terminates when the voltage returns to normal operating conditions.

B. CONTROL STRATEGIES AND ALGORITHMS OF DVR

The detection of voltage disturbances is the major emphasis of the DVR's control system. Specifically, with sensitive loads, the detecting system should be fast enough to identify the voltage disturbance accurately for the assessment of DVR performance [20], [45]. As shown in Figure 2, various methods for voltage disturbance detection have been proposed, including RMS, Peak Value, DFT, Fourier Transform (FT), Wavelet Transform (WT), Windowed Fast FT (WFFT), ABC to DQ axis transformation, KF, Phase-Locked Loop (PLL), and SRF [28], [46]. The benefits and drawbacks of the most serious voltage disturbance detection techniques are provided in Table 1.

C. PROPOSED SYSTEM DESCRIPTION

The proposed configuration shown in Figure 3 includes a supply (grid) voltage with grid impedance, a three-phase load, an injection transformer, and the DVR system. The DVR system comprises a Voltage Source Inverter (VSI) powered by a DC power source with a dc link capacitor and a harmonic passive filter. A three-phase balanced, and unbalanced load is considered in this system [16], [47], [48].

TABLE 1. Voltage disturbance detection techniques benefits and weakness.

Detection Method	Benefits	Weaknesses
Peak Value [42]	0.25 cycle delay in identifying sags/swells.	Pass over noise, difficult to extract phase angle
Discrete Fourier [43]	Sags/swells recognition, harmonic distortion	Requires stationary signal, high Calculations (one cycle for perfect sag/swell value and phase data),
Root Mean Square[6]	Identifies start-/end- of sags/swells, simple, fast	Fails to detect the frequency, harmonic, and phase angle
Fast Fourier Transformation [44]	Quicker than DFT, identifies phase angle shifts, harmonic distortion, precision	Requires stationary signal, integer sample numbers
Phase Locked Loop[24]	Sags/swells recognition, phase angle	Requires time delay upward half-cycle, difficult to control incompatible for single-phase systems, fails to Identify the imbalance of sags/swells voltage
Synchronously Rotating Frame [49]	Fit for three-phase Very short time for detection	
Wavelet Transform[50]	Ease of use time and frequency data	Requires accurate choice of wavelet model, need a delay associated to wavelet models
Kalman Filter [29]	Ideal recognition of voltage sags/swells, solid for working with linear structures	Requests enhanced KF for non-linear structures

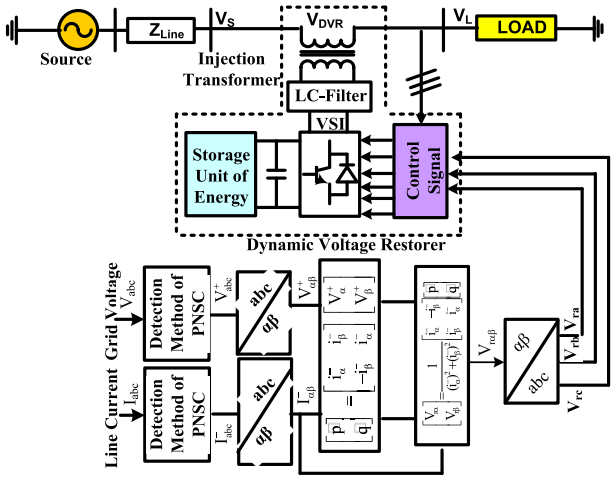

FIGURE 3. Proposed system configuration.

III. INSTANTANEOUS REACTIVE POWER CONTROL TECHNIQUE

Generalized Theory of the Instantaneous Reactive Power in Three-Phase Circuits," also known as "Theory of Instantaneous Real Power and Imaginary Power," or "Theory of Instantaneous Active Power and Reactive Power," or "Theory of Instantaneous Power," or simply "PQ Theory," was proposed by Akagi *et al.* in 1983 for the control of active filters in three-phase power systems. The idea was first formulated for three-phase, three-wire systems, with a brief mention of neutral wire systems. Later, it was expanded to include three-phase four-wire systems (phases a, b, c, and neutral wire) [6], [29].

A. PQ THEORY

PQ theory is a time-domain representation of instantaneous power. This theory is based on Clarke's Transformation. The voltage and current are transformed from abc coordinates to $\alpha\beta 0$ coordinates. This method consists of a real matrix that transforms three-phase voltages and currents into the $\alpha\beta 0$ stationary reference frames [5], [50]. With the help of Clarke's transformation, the voltages and current can be related in terms of abc and $\alpha\beta 0$ as follows:

$$\begin{bmatrix} V_0 \\ V_\alpha \\ V_\beta \end{bmatrix} = \sqrt{\frac{2}{3}} \begin{bmatrix} \frac{1}{\sqrt{2}} & \frac{1}{\sqrt{2}} & \frac{1}{\sqrt{2}} \\ 1 & -\frac{1}{2} & -\frac{1}{2} \\ 0 & \frac{\sqrt{3}}{2} & -\frac{\sqrt{3}}{2} \end{bmatrix} \begin{bmatrix} V_a \\ V_b \\ V_c \end{bmatrix} \tag{1}$$

And the three phase abc currents to $\alpha\beta 0$

$$\begin{bmatrix} I_0 \\ I_\alpha \\ I_\beta \end{bmatrix} = \sqrt{\frac{2}{3}} \begin{bmatrix} \frac{1}{\sqrt{2}} & \frac{1}{\sqrt{2}} & \frac{1}{\sqrt{2}} \\ 1 & -\frac{1}{2} & -\frac{1}{2} \\ 0 & \frac{\sqrt{3}}{2} & -\frac{\sqrt{3}}{2} \end{bmatrix} \begin{bmatrix} I_a \\ I_b \\ I_c \end{bmatrix} \tag{2}$$

The instantaneous active (P), reactive(Q), and zero sequence instantaneous power (P_0), can be represented in $\alpha\beta 0$ of instantaneous phase voltage and current values using the following matrix:

$$\begin{bmatrix} P_0 \\ P \\ Q \end{bmatrix} = \begin{bmatrix} V_0 & 0 & 0 \\ 0 & V_\alpha & V_\beta \\ 0 & V_\beta & -V_\alpha \end{bmatrix} \begin{bmatrix} I_0 \\ I_\alpha \\ I_\beta \end{bmatrix} \tag{3}$$

The instantaneous three phase active power can be represented by using $\alpha\beta 0$ or abc components of voltage, current as shown in following equation

$$P = V_\alpha I_\alpha + V_\beta I_\beta + V_0 I_0 = V_a I_a + V_b I_b + V_c I_c \tag{4}$$

In balanced three phase system zero sequence components of voltage and current V_0 and I_0 can be neglected then the instantaneous three phase active power is:

$$P = V_\alpha I_\alpha + V_\beta I_\beta \tag{5}$$

Similarly, the instantaneous reactive power (Q) in $\alpha\beta$ system can be represented as

$$Q = V_\beta I_\alpha - V_\alpha I_\beta \tag{6}$$

From above two equations both P and Q can be represented in matrix form

$$\begin{bmatrix} P \\ Q \end{bmatrix} = \begin{bmatrix} V_\alpha & V_\beta \\ -V_\beta & V_\alpha \end{bmatrix} \begin{bmatrix} I_\alpha \\ I_\beta \end{bmatrix} \tag{7}$$

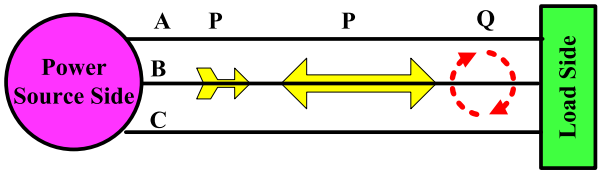

FIGURE 4. Power components of PQ scheme.

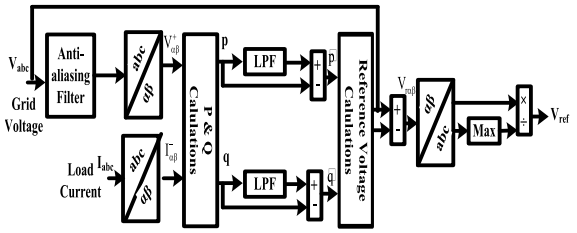

FIGURE 5. Traditional PQ method.

As PQ control technique is intrinsically a 3Φ system, used in with or without a neutral line and balanced or unbalanced. it can be implemented in both steady-state and transient state conditions. It concedes two control strategies, one constant instantaneous power and another is sinusoidal supply current [5], [21]. The power components of the PQ scheme are shown in Figure 4.

B. THE TRADITIONAL PQ CONTROL TECHNIQUE

Figure 5 shows the control model for generating V_{ref} using Traditional PQ. Where the three-phase voltage and Load current are measured. The three-phase grid voltage is sensed and processed through an antialiasing filter and then $\alpha\beta$ positive components of grid voltage ($V^{+}_{\alpha\beta}$) is obtained as given in equation (1). Simultaneously the load current is measured and $\alpha\beta$ negative component of load current $I^{-}_{\alpha\beta}$ is obtained as shown in equation (2). Both the components are processed to calculate the real (P) and reactive power (Q) using equations (5) and (6), later P, and Q are processed through a low pass filter for the generation of real and reactive power in $\alpha\beta$ components where with reference voltage calculation block and inverse Clark's transformation the voltage reference V_{ref} is generated.

C. THE MODIFIED PQ TECHNIQUE

This improved method refers to the generation of a reference signal for compensating the power quality issues. This reference depends on the grid voltage and negative sequence component of load current. Power quality concerns like voltage sag, swell, load change, harmonic impact, balance, and unbalanced load induces the load current negative sequence component. To obtain the compensation, there are two issues firstly the magnitude of the compensation, and secondly the phase of the reference signal which is locked with the grid voltage. For the magnitude of the compensation power, the load current negative sequence component has to be evaluated. The magnitude of the compensating power is corresponding to the level of the negative sequence component of the load current which is given by the following equation.

$$i^{-}_{abc}(t)f_n = \begin{bmatrix} i^{-}_a(t) \\ i^{-}_b(t) \\ i^{-}_c(t) \end{bmatrix} \tag{8}$$

The phasing of the reference signal is obtained by using the source side voltage by computing it from the positive sequence component of the grid voltage. It is evaluated with the following equation

$$V^{1}_{abc}(t)f_n = \begin{bmatrix} V^{+}_a(t) \\ V^{+}_b(t) \\ V^{+}_c(t) \end{bmatrix} \tag{9}$$

To obtain the phasing, amplitudes of positive sequence components are normalized at the desired value using the maximum amplitude detection as following:

$$v^{+}(t) = |V_{ref}| \frac{v^{+}(t)}{v^{+}(t)} \tag{10}$$

The grid voltages ($\boldsymbol{v_{abc}}$) and the load currents ($\boldsymbol{i_{abc}}$) are measured in per unit (pu). Then Clark's transformation is used to transform the three-phase positive sequence components of $\boldsymbol{v_{abc}}$ and negative sequence components of the currents signals into two signals (V^{+}_{α}, V^{+}_{β}) and (I^{-}_{α}, I^{-}_{β}) using:

$$\begin{bmatrix} V^{+}_{\alpha} \\ V^{+}_{\alpha} \end{bmatrix} = \sqrt{\frac{2}{3}} \begin{bmatrix} 1 & -\frac{1}{\sqrt{2}} & -\frac{1}{\sqrt{2}} \\ 0 & \frac{\sqrt{3}}{2} & -\frac{\sqrt{3}}{2} \end{bmatrix} \begin{bmatrix} V^{+}_a \\ V^{+}_b \\ V^{+}_c \end{bmatrix} \tag{11}$$

$$\begin{bmatrix} I^{-}_{\alpha} \\ I^{-}_{\beta} \end{bmatrix} = \sqrt{\frac{2}{3}} \begin{bmatrix} 1 & -\frac{1}{\sqrt{2}} & -\frac{1}{\sqrt{2}} \\ 0 & \frac{\sqrt{3}}{2} & -\frac{\sqrt{3}}{2} \end{bmatrix} \begin{bmatrix} I^{-}_a \\ I^{-}_b \\ I^{-}_c \end{bmatrix} \tag{12}$$

To obtain the instantaneous active and reactive powers, α and β components of positive sequence voltage and negative sequence currents vectors are evaluated using equations (11) and (12).

The instantaneous active and reactive power ($\tilde{p}$ and $\tilde{q}$); in terms of positive sequence components of grid voltage and negative sequence components of the load currents; are calculated as:

$$\tilde{p} + j\tilde{q} = v^{+}_{\alpha} i^{-}_{\alpha} + v^{+}_{\beta} i^{-}_{\beta} - jv^{+}_{\alpha} i^{-}_{\beta} + jv^{+}_{\beta} i^{-}_{\alpha} \tag{13}$$

The above equation in the matrix form can be expressed as:

$$\begin{bmatrix} \tilde{p} \\ \tilde{q} \end{bmatrix} = \begin{bmatrix} i^{-}_{\alpha} & i^{-}_{\beta} \\ -i^{-}_{\beta} & i^{-}_{\alpha} \end{bmatrix} \begin{bmatrix} V^{+}_{\alpha} \\ V^{+}_{\beta} \end{bmatrix} \tag{14}$$

The inverter of the DVR is supplied from a constant DC power source. consequently, there is no need to control dc voltage. The reference voltages used to control the inverter can be obtained by the inverse of the above matrix as follow:

$$\begin{bmatrix} V_{r\alpha} \\ V_{r\beta} \end{bmatrix} = \frac{1}{(i^{-}_{\alpha})^2 + (i^{-}_{\beta})^2} \begin{bmatrix} i^{-}_{\alpha} & -i^{-}_{\beta} \\ i^{-}_{\beta} & i^{-}_{\alpha} \end{bmatrix} \begin{bmatrix} \tilde{p} \\ \tilde{q} \end{bmatrix} \tag{15}$$

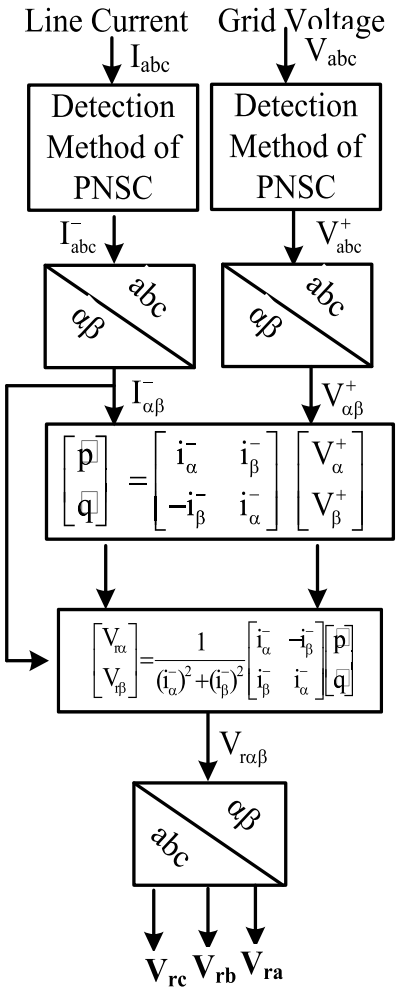

FIGURE 6. Block diagram of the modified PQ method.

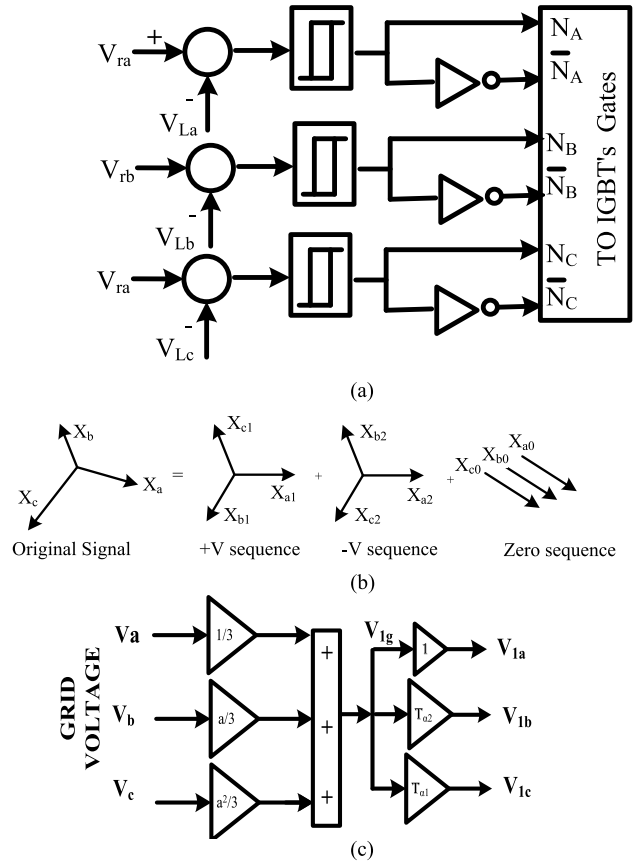

FIGURE 7. (a) Hysteresis voltage controller. (b) Symmetrical components (X: grid voltages or load currents. (c) Extraction method of positive components of grid voltage.

These reference signals are then transformed into abc coordination using inverse Clark's transformation as:

$$\begin{bmatrix} V_{ra} \\ V_{rb} \\ V_{rc} \end{bmatrix} = \sqrt{\frac{2}{3}} \begin{bmatrix} 1 & 1 \\ -\frac{1}{2} & \frac{\sqrt{3}}{2} \\ -\frac{1}{2} & -\frac{\sqrt{3}}{2} \end{bmatrix} \begin{bmatrix} V_{r\alpha} \\ V_{r\beta} \end{bmatrix} \tag{16}$$

Figure 6 explains the proposed method for voltage reference generation.

D. HYSTERSIS VOLTAGE CONTROL

The switching signals for the voltage source inverter are generated using a hysteresis voltage controller. The load voltage references are compared with the measured load voltages. The error signals are then processed through the hysteresis band. This scheme can be seen in Figure 7. A hysteresis voltage controller has the benefits of effective dynamic response, superior precision, cheap cost, and ease of implementation, the hysteresis controller is favored over standard controllers such as PWM and SVPWM [51]. The hysteresis control approach overcomes the problems of classic systems such as switching losses with the high switching frequency, electromagnetic interference difficulties owing to higher-order harmonics, and a reduction in available voltage [2], [52].

Actual load voltages are compared to the produced voltage references. Figure 8 shows how the hysteresis band is used to process the difference between reference and actual voltage values to create the firing signals of inverter IGBT switches.

Asymmetrical components (positive and negative sequence components) appear in the system grid voltages and load currents through abnormal operating. The proposed control system is designed to extract the positive sequence component from the grid voltage and the negative sequence component from the load current. The active and reactive power are calculated using the positive grid voltage and negative sequences of the load current using the equation (11), (12). To generate the reference of Compensating voltages, equation (15) is used to produce the reference voltage in ($\alpha\beta$) coordinate system, these ($\alpha\beta$) are transformed to abc coordinate system using inverse Clarke transformation by equation (16). Hysteresis voltage control is used to generate firing signals for VSI switches by comparing reference voltages to real load voltages. This reference generation scheme enables the control system to compensate for the load voltage by identifying

TABLE 2. Parameters of the system under TEST.

	Parameters	Values
Source	voltage of Grid	100 V_{peak}
	Frequency	50 Hz
	DC power source	280 V
VSI	Switching frequency (SW)	10 kHz
Load	Load parameters	S_L=1 kVA, 0.5kVA
DVR	Injection transformer	1:1 ratio, 10 kVA
	L_f, C_f, R_f	3 mH, 100 μF, 0.5 □

the negative sequence components under any condition of power quality issues like voltage sag, swell, load unbalanced harmonics, phase failure for a short time, and load change.

This improved PQ control method does not include the phase-locked loop (PLL), conventional PI controller, and filters for the generation of voltage references, leading to the instantaneous, continuous and fast dynamic response for compensating the load voltage.

E. PARAMETERS OF THE SYSTEM UNDER TEST

F. POSITIVE SEQUENCE COMPONENTS CALCULATIONS

Figure 7b shows the positive, negative, and zero components under abnormal situations. The approach pursues to extract the positive sequence components of grid voltage which are three phasors with identical magnitudes that are displaced by 120° and rotate anticlockwise [30].

This method is established on time domain. The phase angle can be expressed in a time interval as follow:

$$t_{ph} = \frac{\text{phase angle}}{360^\circ} \times \frac{1}{f} \tag{17}$$

where t_{ph} is the phase shift (Φ) in time between two phases, f is the fundamental frequency. The symmetrical components of three-phase ungrounded voltages system can be expressed as:

$$\begin{aligned} \mathbf{V_{abc}}\,(\mathbf{t}) &= \begin{bmatrix} V_a \cos(\omega t + \Phi) \\ V_b \cos\left(\omega t + \Phi - \frac{2\pi}{3}\right) \\ V_c \cos\left(\omega t + \Phi + \frac{2\pi}{3}\right) \end{bmatrix} \\ &= V_1 \begin{bmatrix} \cos(\omega t + \Phi^1) \\ \cos\left(\omega t + \Phi^1 - \frac{2\pi}{3}\right) \\ \cos\left(\omega t + \Phi^1 + \frac{2\pi}{3}\right) \end{bmatrix} \\ &\quad + V_2 \begin{bmatrix} \cos(\omega t + \Phi^2) \\ \cos(\omega t + \Phi^2 - \frac{2\pi}{3}) \\ \cos(\omega t + \Phi^2 + \frac{2\pi}{3}) \end{bmatrix} \end{aligned} \tag{18}$$

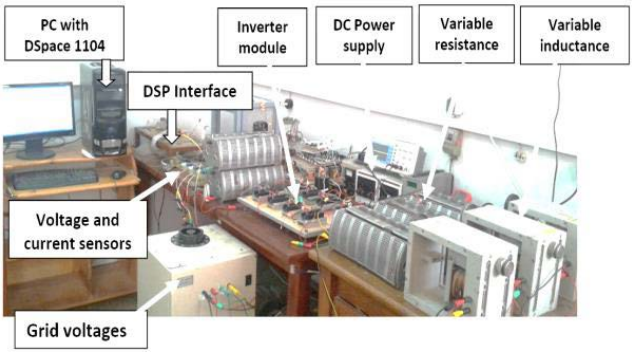

FIGURE 8. Experimental setup.

The symmetrical components equations are converted to time-domain to separate the positive sequence components as follow:

$$V_{1abc}\,(t) = \begin{bmatrix} V_{1a}\,(t) \\ V_{1b}\,(t) \\ V_{1c}\,(t) \end{bmatrix} = \begin{bmatrix} V_1\,(t) \\ V_1\,(T_{\alpha 1}) \\ V_1\,(T_{\alpha 2}) \end{bmatrix} \tag{19}$$

$$V_1\,(t) = \frac{1}{3}[V_a\,(t) + V_b\,(T_{\alpha 1}) + V_c\,(T_\alpha)] \tag{20}$$

$$t_{(\alpha 1)} = \frac{240^\circ}{360^\circ} * \frac{1}{f} \quad t_{\alpha 2} = \frac{120^\circ}{360^\circ} * \frac{1}{f} \tag{21}$$

wherever V_1 (t) is the positive sequence component in time domain interpretation of the 3-phase grid voltages, $T_{\alpha 1}$ and $T_{\alpha 2}$ are the time phase angle shift of the symmetrical component. Wherever, $T_{\alpha 1}$= t+t_{ph} − $t_{\alpha 1}$ and $T_{\alpha 2}$= t+t_{ph} + $t_{\alpha 2}$. Figure 7c shows the removal of grid voltage negative sequence component.

IV. EXPERIMENTAL SETUP

The experimental setup for the proposed DVR system is shown in Figure 8. It is comprised of two circuits: one for the power and the other for control. The full experimental circuit consists of a three-phase AC voltage source, a transformer, VSI powered by a DC power source, and a 1kVA load. The control circuit is based on the digital signal processing type dSPACE (DS1104) to execute the proposed system, which was employed using Matlab/Simulink. LV25-P voltage transducer circuit is used to measure the supply and load voltages. LA25 current sensor circuits are used to sense the load currents. Measured signals are scaled down to 10V before being given as inputs to the DS1104 board to fulfil the control board's requirements.

The system parameters are presented in Table 4.

V. RESULTS AND DISCUSSIONS

To verify the proposed modified PQ control system for reference generation the complete system model is implemented in two different ways. Firstly, MATLAB simulation of the system based on "mathematical equations 1 to 16" is implemented and secondly experimental setup using "DSPACE DS1104 control board". Different scenarios of severe power quality conditions are extracted to verify and validate the

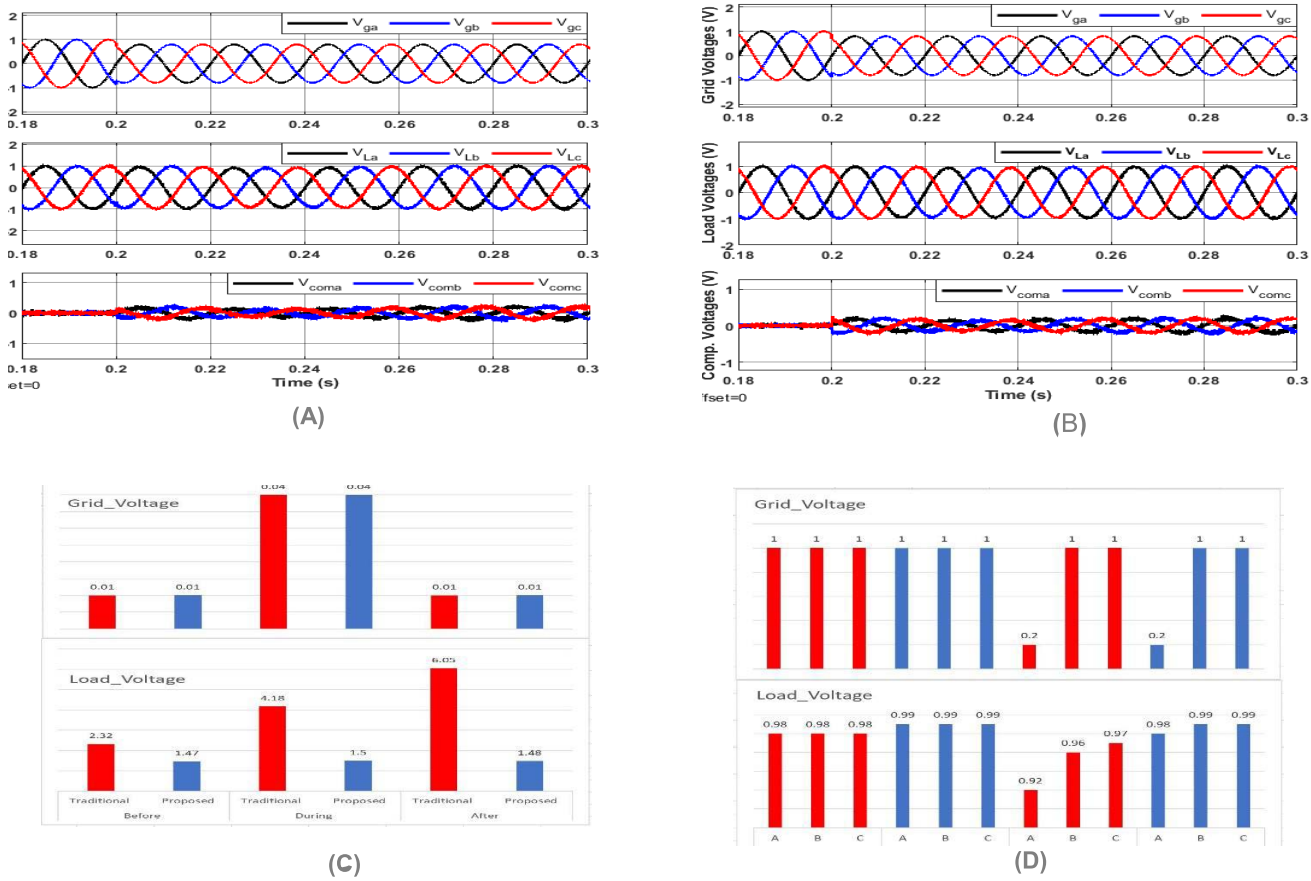

FIGURE 9. Simulation results of grid voltages, load voltage and dvr voltages (a) traditional PQ (b) modified PQ (c) THD of voltage (d) voltage amplitude under balanced 3ϕ load voltage sag of 20%.

efficacy of the proposed PQ scheme. The different scenarios of balanced, unbalanced, (sag and swell) and load reduction are considered and discussed in this section.

A. CASE 1: BALANCED LOAD CONDITION

1) 20% SAG OF GRID VOLTAGE IN BALANCED LOAD CONDITION

In this case of balanced load condition, the three-phase grid voltage is affected by a 20% sag. Figure 9A shows the simulation results of the grid, load and compensating voltage for the balanced load voltage scenario using the conventional PQ technique. Here, the sag is starting at the instant of 0.2 seconds (s). With conventional PQ, it is observed that the load voltage waveform is distorted, and the associated compensating voltage is injected at almost the same instant of 0.2S. Figure 9B shows simulated waveforms of Gird voltage, load voltage, and appropriate compensating voltage with the proposed PQ control with 20% sag of grid voltage under balanced load conditions. Under this balanced condition, the compensating voltage is injected instantaneously at 0.2s. The load voltage waveform shows very low distortion and a good voltage profile when the proposed PQ control is used to compensate for 20 percent sag.

The comparison of the obtained total harmonic distortion (THD) in grid voltage and load voltage for the traditional and proposed PQ technique is shown in Figure 9C. The THD value is measured before, during, and after compensation conditions and compared between the traditional and proposed PQ techniques. It is observed that for grid voltage both THDs for traditional and proposed methods are showing similar values. Whereas for load voltage, the THD is much improved with the proposed PQ method for all the conditions of before, during, and after compensation.

The amplitude of the grid voltage and the load voltages are measured in per unit (PU), and compared before and during compensation for all considered cases. The comparison for amplitude with traditional and proposed PQ methods is shown in Figure 9D. It can be observed that the grid voltage with traditional and proposed PQ methods is the same. Whereas a decent load voltage is maintained nearer to 1 by the proposed PQ method. The traditional PQ method load voltages were not well compensated as the modified PQ method under conditions before and during compensation.

Figure 10A shows the experimental results using the traditional PQ control technique implemented for a balanced 20% sag scenario. It can be observed that the load voltage

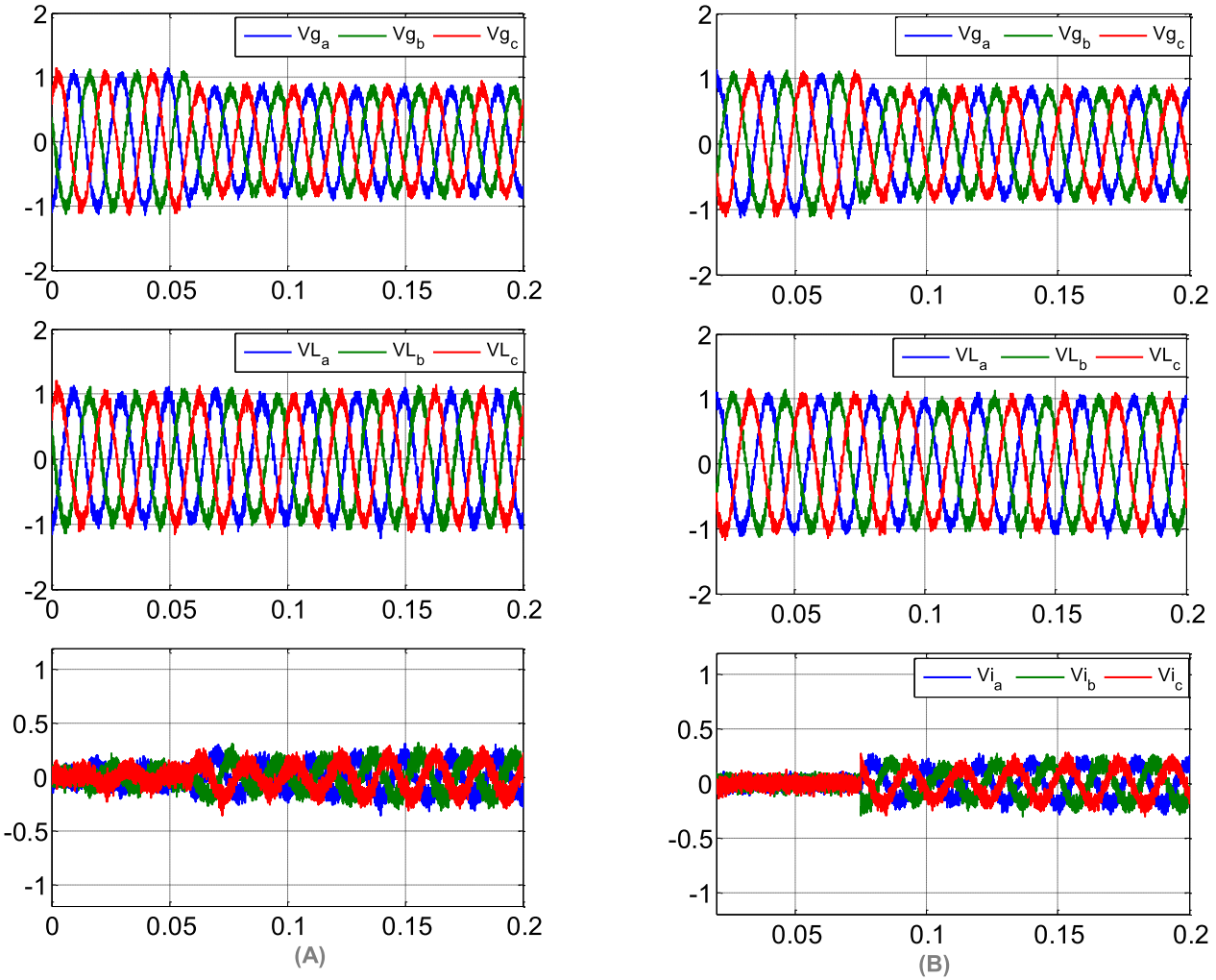

FIGURE 10. Experimental results of grid voltages, load voltage and DVR voltages (a) traditional PQ (b) modified PQ under balanced 3ϕ load voltage sag of 20%.

has distortions even after compensating voltage is injected at 0.075 s. The complete compensation is not obtained with the traditional PQ. On the other hand, the experimental results of the proposed PQ control for 20% sag under balanced conditions provide an instantaneous injection of compensating voltage at 0.075 s, leading to enhanced load voltage quality, as illustrated in Figure 10B.

The per-unit (pu) load voltage and load frequency of the traditional and proposed PQ techniques are compared in Figure 11 under the scenario of a 20% balanced sag. The load voltage sags by 0.2 pu starting at 0.2 s to 0.28 s with the traditional PQ approach. Whereas the load voltage sags by less than 0.1 PU between 0.2 s to 0.26 s and then returns to the nominal value of 1 PU, with the improved PQ technique. This demonstrates the proposed technique's effectiveness and quick settlement to the nominal voltage value. The load frequency has affected with a small change of less than 0.2 Hz from 0.2 s to 0.28 s, with a maximum change of 0.2 Hz at 0.23 s, using the traditional PQ approach. With modified PQ,

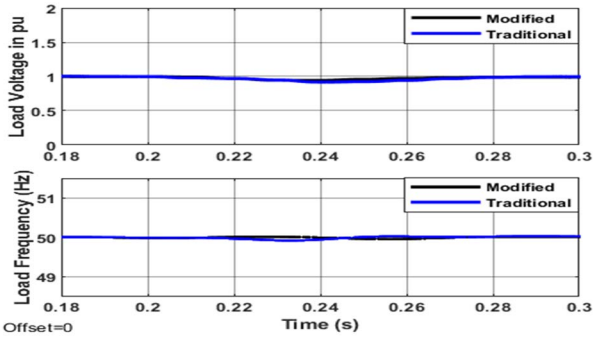

FIGURE 11. [Upper] PU load voltage, [lower] load frequency under balanced 3ϕ load voltage sag of 20%.

the change in load frequency is very less of about 0.1 Hz from 0.2 s to 0.27 s with a maximum change of 0.1 Hz at 0.23 s. Hence This illustrates the effectiveness of the improved PQ approach.

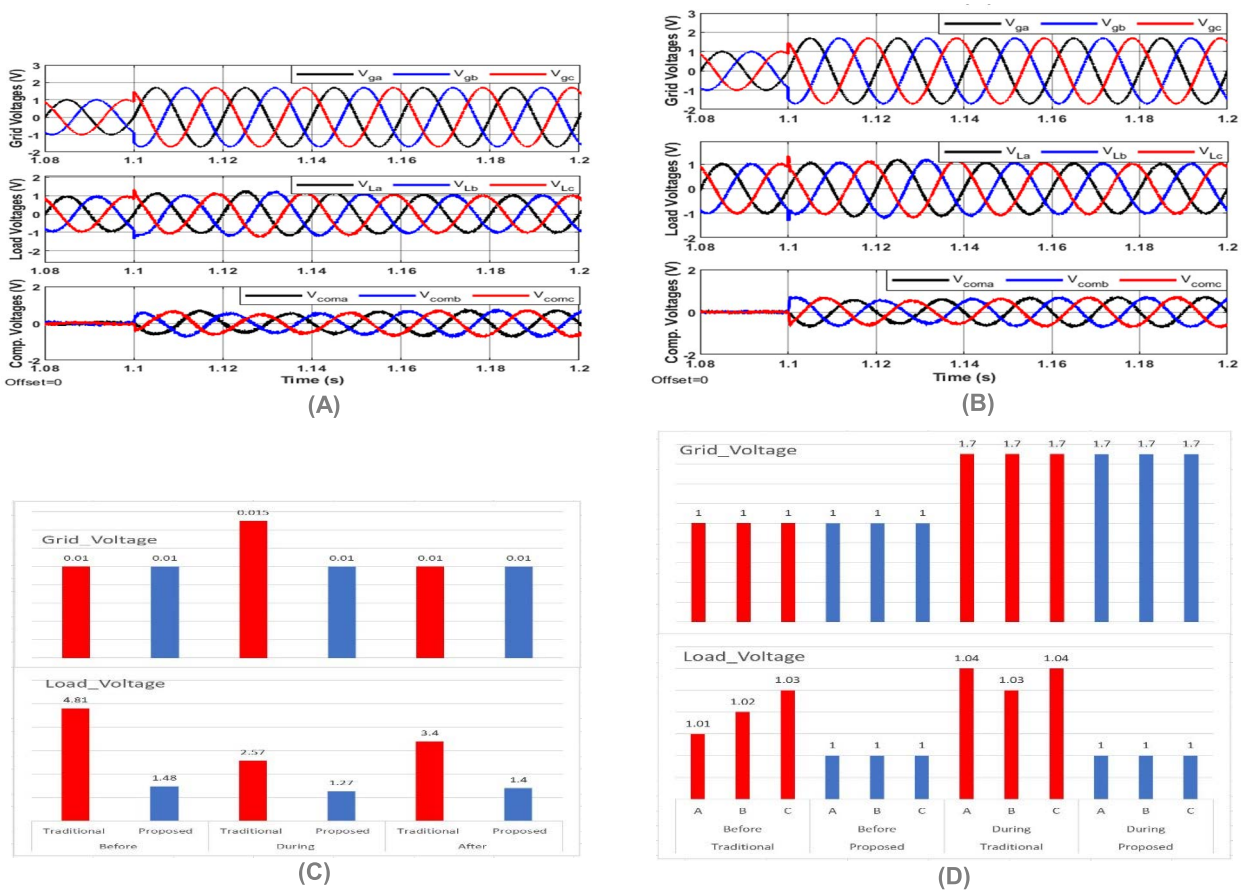

FIGURE 12. Simulation results of grid voltages, load voltage and DVR voltages (a) traditional PQ (b) modified PQ (c) THD of voltage (d) voltage amplitude under balanced 3ϕ load voltage swell of 70%.

2) 70% SWELL OF GRID VOLTAGE IN BALANCED LOAD CONDITION

Figure 12A represents the simulation results of the grid, load, and compensating voltages with traditional PQ under balanced load conditions with 70% swell in grid voltage. It can be observed that the swell in the system is initiated at 1.1 s. The corresponding compensation voltage is also injected at 1.1 s promptly. Though with the instantaneous injection of the compensation voltage the load voltage is severely distorted with still the load voltage having a swell of around 20% from 1.12 s to 1.14 s. Figure 12B illustrates the simulation results of the modified PQ where the compensation voltage is injected instantaneously at 1.1 s. In this case, the load voltage is compensated to the maximum with a very low swell after compensation of around 10% between 1.12 s to 1.14 s. The load voltage has shown a fair improvement in the voltage profile and excellent compensation with the proposed PQ control technique.

The comparison of total harmonic distortion (THD) in grid voltage and load voltage for traditional and proposed PQ techniques with 70% swell under balanced conditions is shown in Figure 12C. It is observed for grid voltage, both THDs with traditional and proposed methods are showing almost equal values for before and after compensation. Whereas for load voltage, the THD is much improved with the proposed PQ method for all the conditions of before, during, and after compensation.

The comparison of the amplitude of grid voltage and load voltage before and during with traditional and Proposed PQ methods is shown in Figure 12D. It can be observed that the grid voltage measured with traditional and Proposed PQ methods are same. With the traditional PQ method load voltages are slightly greater than one in all the phases under conditions before and during compensation. Whereas a perfect load voltage of 1 pu is maintained by the proposed PQ method.

Figure 13A shows experimental results of the grid, load, and compensating voltages using the traditional PQ approach for the balanced 70 % swell. Under these conditions, the swell at 0.052 s is observed and instantaneous compensating voltage is injected resulting in a much-distorted load voltage with swells of around 30% still existing in the system from 0.052 s. Figure 13B explains the experimental results of the grid, load, and compensation voltage for the proposed PQ technique. It is observed that the load voltage from 0.052 s has an improved voltage profile with less distortions with

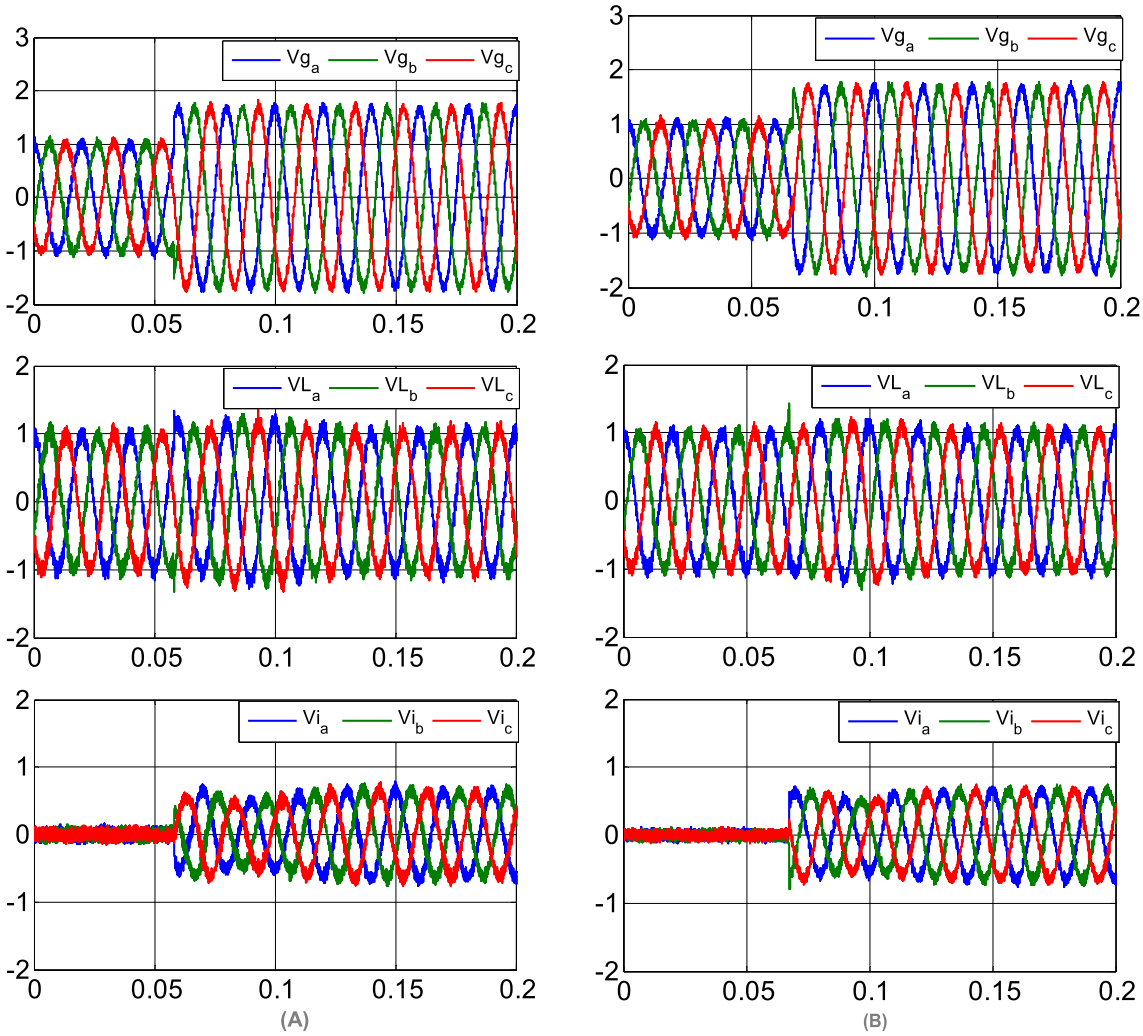

FIGURE 13. Experimental results of grid voltages, load voltage and DVR voltages (a) traditional PQ (b) modified PQ under balanced 3ϕ load voltage swell of 70%.

a low swell of 10% when compared to the traditional PQ technique.

Figure 14 compares the per unit load voltage and frequency of the traditional and proposed PQ techniques under the scenario of 70% swell in a balanced condition. The upper figure illustrates the load voltage has a swell from 1.11 s to 1.18 s with a maximum swell of 1.275 pu at 1.14 s while using the traditional PQ approach. Also explains, with the proposed PQ controller the swell in load voltage observed is from 1.11 s to 1.165 s with a maximum swell of 1.2 pu at 1.12 s which depicts that the proposed PQ controller instantly compensates for the load voltage. Figure 14 lower depicts the load frequency change with the traditional PQ technique as less than 0.2 Hz from 1.12 s to 1.16 s, with a maximum change of 0.2 Hz at 1.135 s, whereas the load frequency change with the proposed PQ approach is less than 0.1 Hz during 1.12 s to 1.15 s with a maximum change of −0.1 Hz at 1.13 s. This illustrates that the improved PQ has very fast capabilities in identifying swell and improving the power quality.

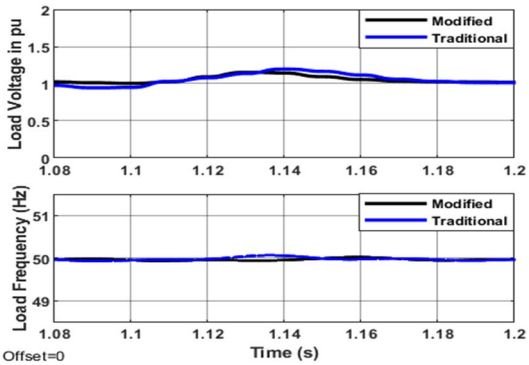

FIGURE 14. [Upper] PU load voltage, [lower] load frequency under balanced 3ϕ load voltage swell of 70%.

B. CASE 2: UNBALANCED LOAD CONDITION

1) 20% SAG OF LOAD VOLTAGE IN UNBALANCED LOAD CONDITION

One of the phases is influenced by a 20% sag in this unbalanced scenario. Figure 15A shows the simulation results

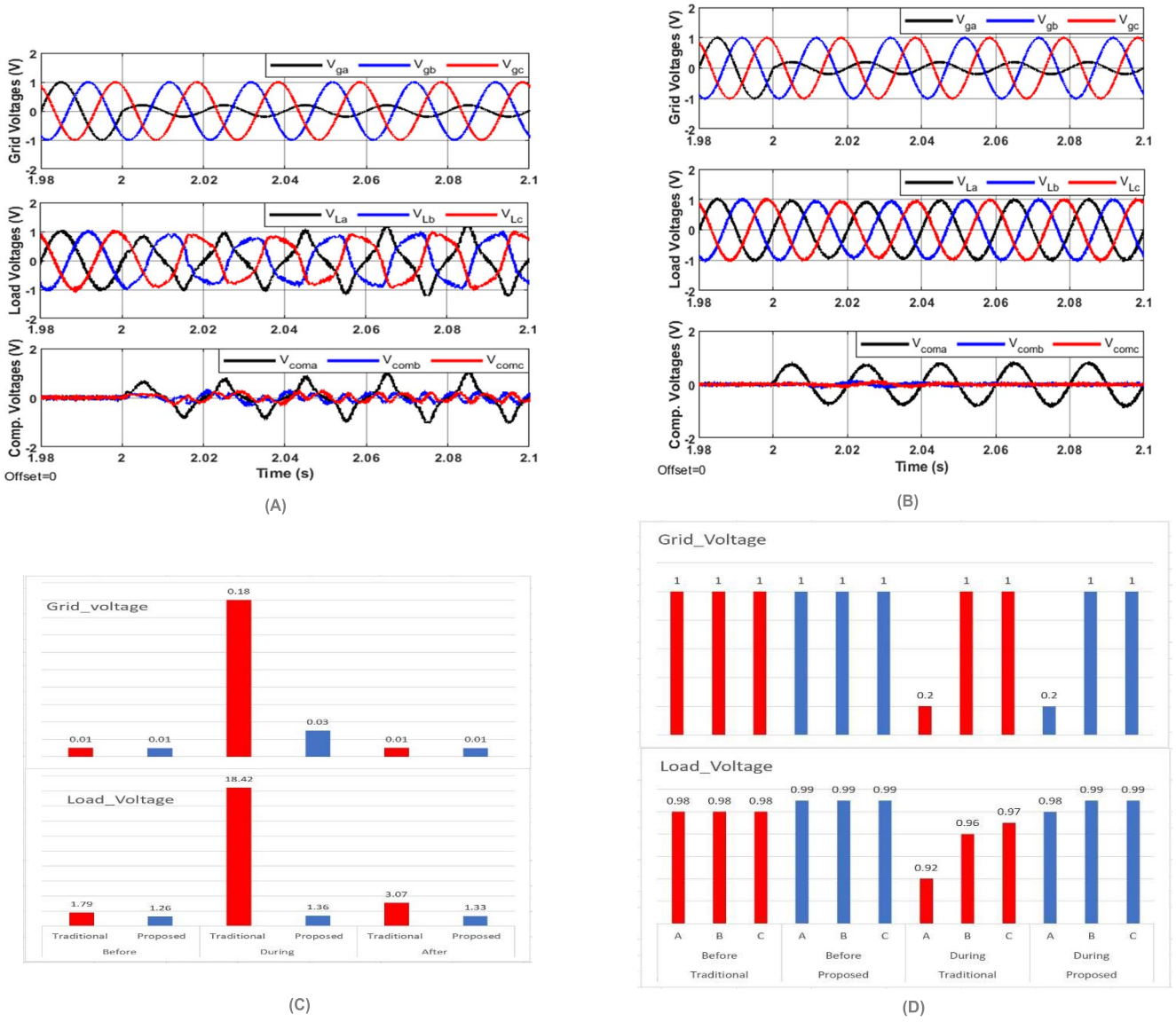

FIGURE 15. Simulation results of grid voltages, load voltage and DVR voltages (a) traditional PQ (b) modified PQ (c) THD of voltage (d) voltage amplitude under unbalanced 3ϕ load voltage sag of 20%.

for this unbalance scenario with grid voltage, load voltage, as well as compensating voltage using traditional PQ. Here, the sag in a single-phase starts at 2 s. The associated compensating voltage is injected almost at the same instant of 2 s. Figure 15B shows simulated waveforms of Gird voltage, load voltage, and appropriate compensating voltage with the proposed PQ control under 20% sag in one phase. It is observed that the load voltage waveform has very low distortion with the initiation of compensation voltage at 2 s. The load voltage waveform shows a good voltage profile when the proposed PQ control is used to compensate for 20% sag in one of the phases.

The comparison of total harmonic distortion (THD) for grid voltage and load voltage with traditional and proposed PQ technique having 70% swell under unbalanced condition is shown in Figure 15C. It is observed for grid voltage, both THDs with traditional and proposed methods are showing nearly equal values for before and after compensation. And in during compensation of grid voltage THD with traditional PQ is 0.18% whereas with proposed PQ the THD value is improved to 0.03%. For load voltage, the THD is much improved with the proposed PQ method for all the conditions of before, during, and after compensation. Especially in ''during compensation'' with traditional PQ THD obtained is 18.42% whereas, with proposed PQ THD in source voltage is improved to 1.35%.

The comparison of the amplitude of grid voltage and load voltage before and during with traditional and Proposed PQ methods is shown in Figure 15D. It can be observed that the grid voltage measured with traditional and Proposed PQ

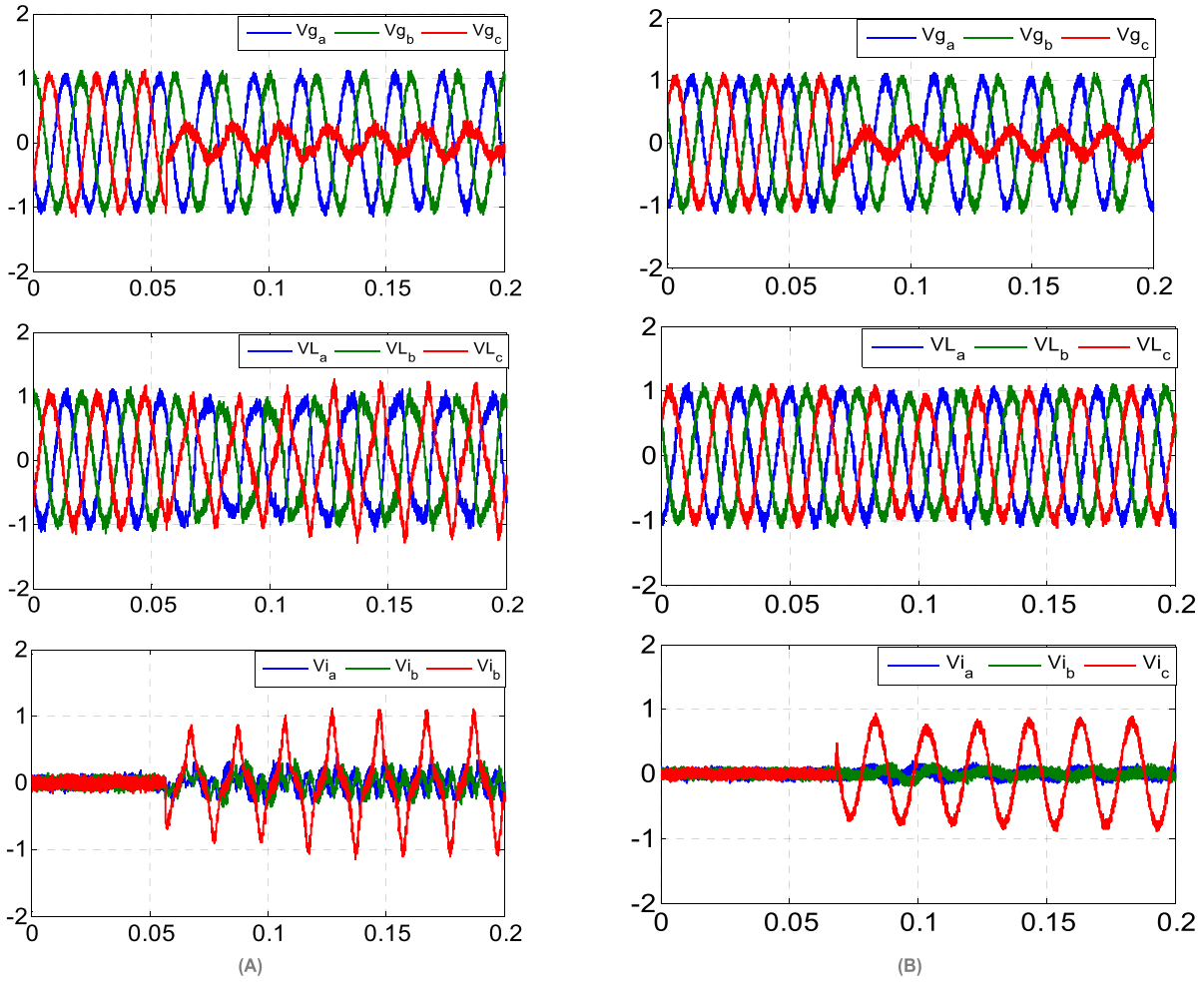

FIGURE 16. Experimental results of grid voltages, load voltage and DVR voltages (a) traditional PQ (b) modified PQ under unbalanced 3ϕ load voltage sag of 20%.

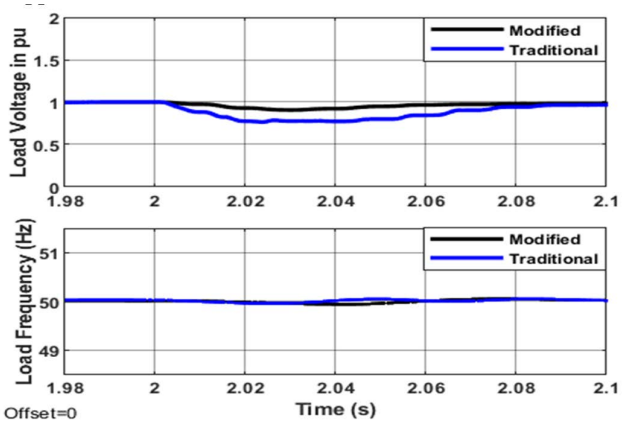

FIGURE 17. [Upper] PU load voltage, [lower] load frequency under unbalanced 3ϕ load voltage sag of 20%.

methods are the same. With the proposed PQ the load voltage had shown a more satisfactory value of nearer to 1pu when compared to the traditional PQ control.

Figure 16A shows the experimental results using traditional PQ control for an unbalanced 20% sag scenario. Figure 16A explains that one of the phases is having sag at 0.053 s and an instantaneous injection of compensating voltage is performed. The resultant load voltage has still some distortion and unbalanced conditions. Figure 16B illustrates the grid, load, and compensation voltage for experimental results of the proposed PQ technique. It can be observed with the instantaneous injection of compensation voltage at 0.053 s the load voltage has improved voltage profile with the proposed PQ method when compared to the traditional PQ.

The per-unit load voltage and load frequency of the traditional and proposed PQ techniques are compared in Figure 17 under the scenario of a 20% unbalanced sag. The load voltage sags by 0.25 pu beginning at 2 s with the traditional PQ approach, but the load voltage sags by less than 0.1 pu between 2.01 s and 2.06 s with the improved PQ technique and then returns to the nominal value of 1 pu. This demonstrates the proposed technique's effectiveness and quick adjustment. The load frequency has a change of 0.2 Hz from 2.04 s to 2.06 s using the traditional PQ approach.

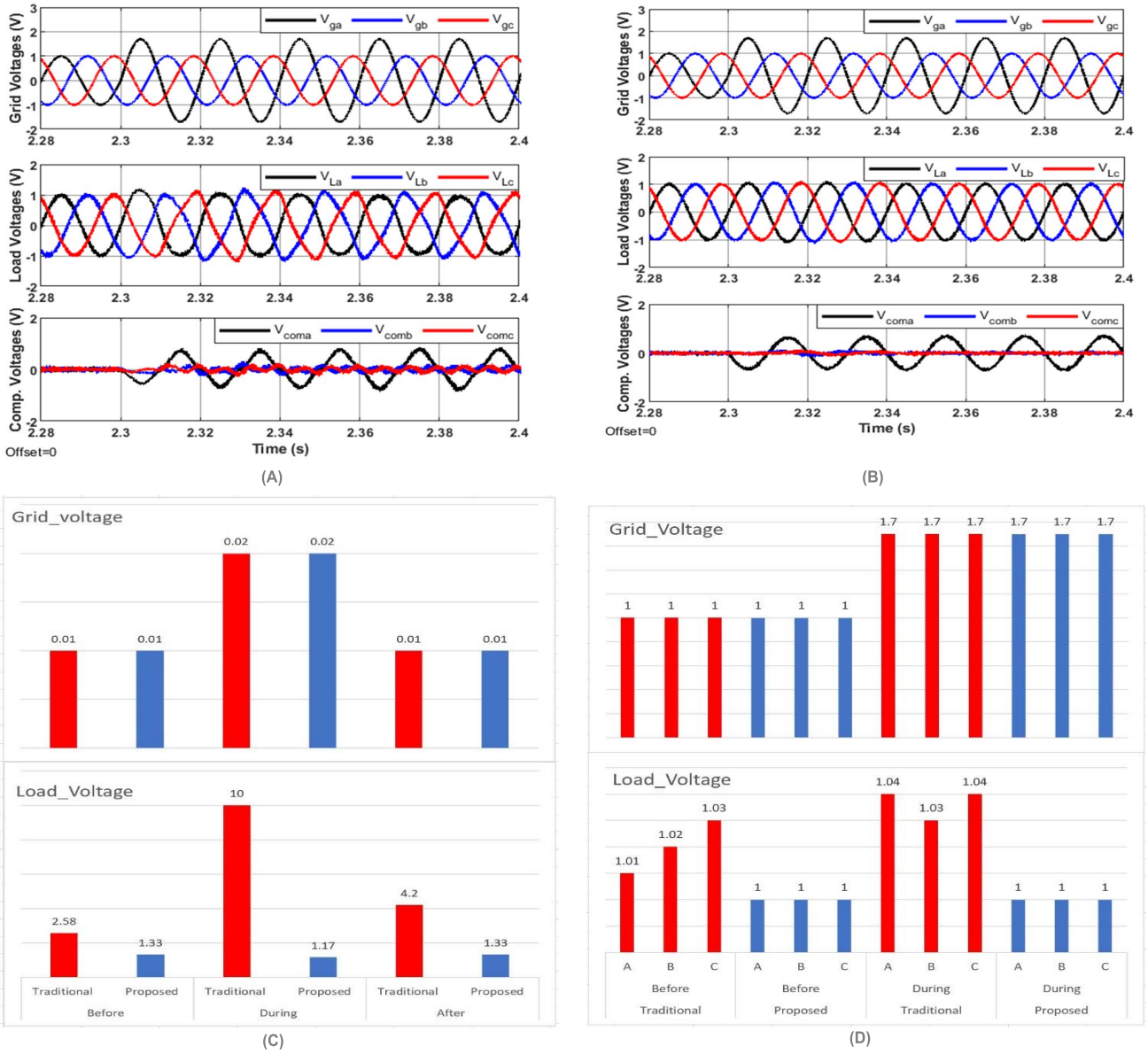

FIGURE 18. Simulation results of grid voltages, load voltage and DVR voltages (a) traditional PQ (b) modified PQ (c) THD of voltage (d) voltage amplitude under unbalanced 3ϕ load voltage swell of 70%.

Whereas, the change in frequency is less than 0.1 Hz from 2.04 s to 2.06 s with a maximum change of 0.1 Hz at 2.05 s. This illustrates the effectiveness of the improved PQ approach.

2) 70% SWELL OF LOAD VOLTAGE IN UNBALANCED LOAD CONDITION

Figure 18A shows the simulation results of the grid, load, and compensating voltages with traditional PQ for an unbalanced condition during a single phase 70% swell. In this case, the load voltage is severely distorted, and the swelled phase still has a slight swell without total compensation. On the other side, by using the proposed PQ control technique, excellent compensation is observed with perfect compensation of voltage. Figure 18B shows simulation results of the grid, load, and compensating voltages using the new PQ approach for an unbalanced single phase 70 % swell.

THD for grid voltage and load voltage with traditional and proposed PQ technique having 70% swell in one phase is shown in Figure 18C. It is observed for grid voltage, both THDs with traditional and proposed methods are displaying similar weights for before, during, and after compensation. For load voltage, the THD is much improved with the proposed PQ method for all the conditions of before, during, and after compensation. The measured THD values with modified PQ are 1.33, 1.17, and 1.33 under before, during, and after compensation respectively.

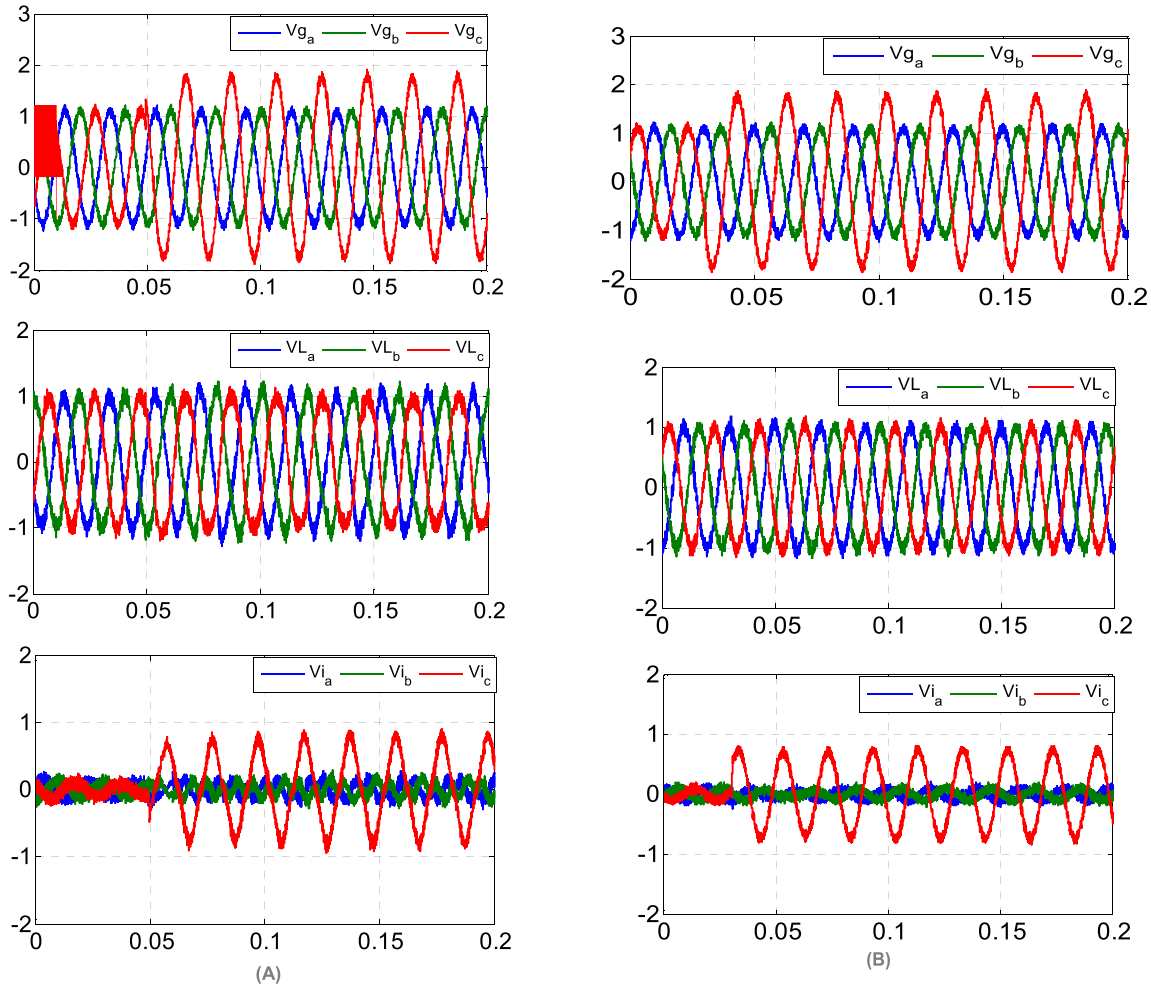

FIGURE 19. Experimental results of grid voltages, load voltage and DVR voltages (a) traditional PQ (b) modified PQ under unbalanced 3ϕ load voltage swell of 70%.

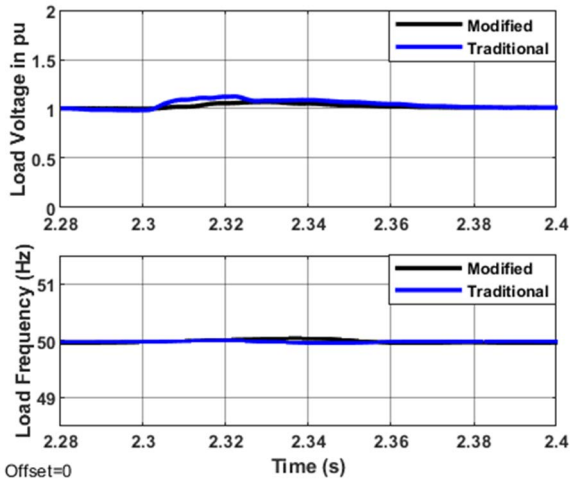

FIGURE 20. [Upper] PU load voltage, [lower] load frequency under ubalanced 3ϕ load voltage swell of 70%.

The comparison of the amplitude of grid voltage and load voltage before and during with traditional and Proposed PQ methods is shown in Figure 18D. It can be observed that the grid voltage measured with traditional and Proposed PQ methods are identical. With the proposed PQ the load voltage had shown suitable voltage amplitudes equal to 1 pu when compared to the traditional PQ control.

Figure 19A illustrates the experimental results of a 70% swell unbalanced three-phase grid using the traditional PQ control strategy. Under these conditions, the load voltage has more distortion and still has swell. The experimental results of the grid, load, and compensating voltage for the proposed PQ technique are shown in Figure 19B. It can be observed that the 70% swell in one phase is observed at 0.05 s. The compensation voltage is injected instantaneously at 0.05 s. The load voltage profile has improved with a completely compensated swell under this proposed PQ control.

Figure 20 compares the per unit load voltage and frequency of the traditional and proposed PQ methods under the scenario of 70% swell. It illustrates the load voltage swells from 2.3 s to 2.36 s with a maximum change of 0.2 pu at 2.32 s while using the traditional PQ approach. Whereas, the proposed PQ controller instantly compensates the voltage to less than 0.1 pu in 2.3 s to 2.35 s. The load frequency change with the traditional DQ technique is less than 0.075 Hz from

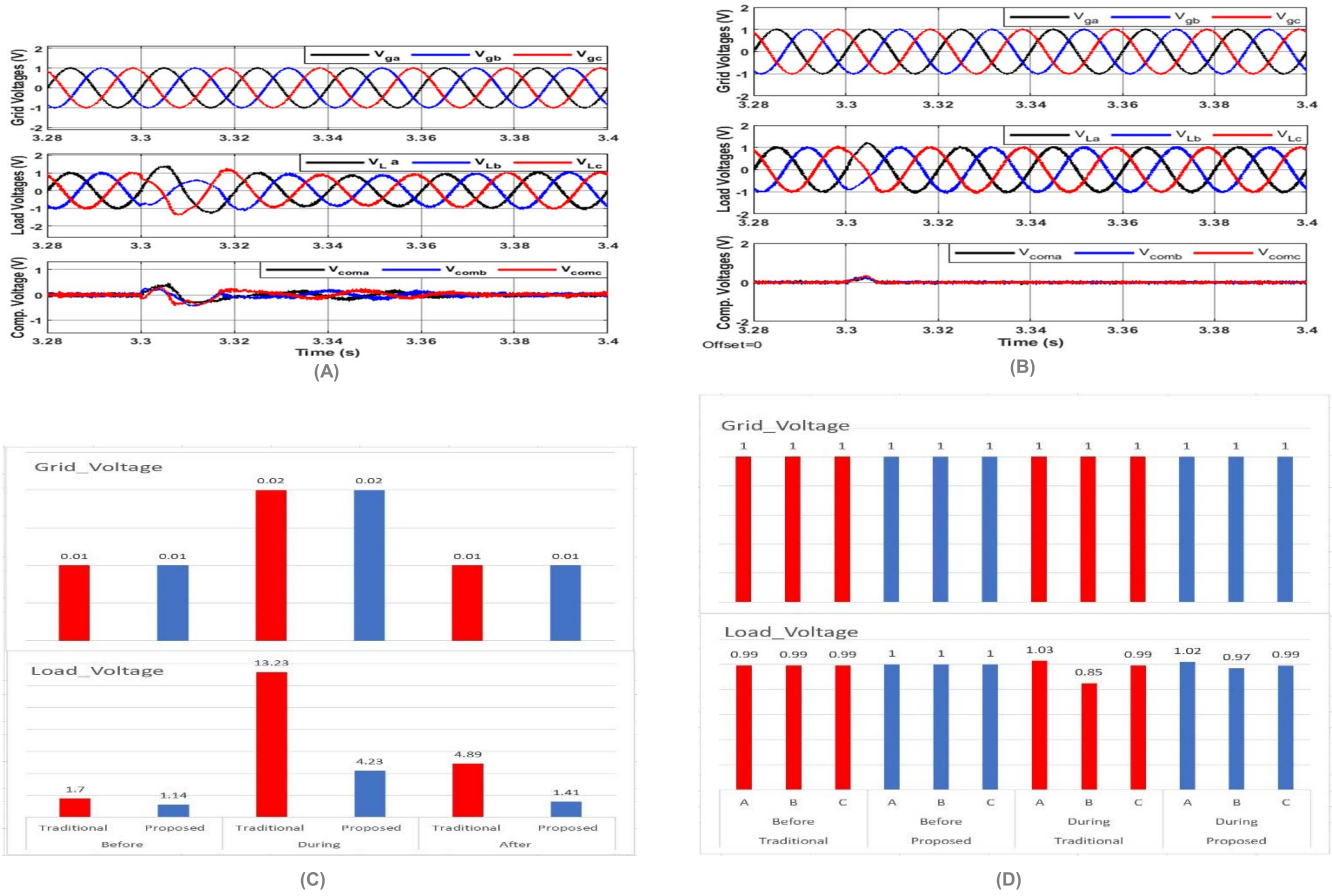

FIGURE 21. Simulation results of grid voltages, load voltage and DVR voltages (a) traditional PQ (b) modified PQ (c) THD of voltage (d) voltage amplitude under 50% load change.

2.32 s to 2.35 s, with a maximum change of 0.1 Hz at 2.335 s, whereas the load frequency change with the proposed PQ approach is less than 0.05 Hz during 2.32 s to 2.34 s with a maximum change of 0.05 Hz at 2.33 s. This illustrates that the improved PQ has very fast capabilities in identifying and compensating the swell.

C. 50% REDUCTION IN THE LOAD

In this scenario, the system is subjected to a 50% drop in load. The simulation waveforms of the grid, load, and compensated voltages, using the traditional PQ and improved PQ are shown in Figures 21A and 21B respectively. It can be observed that the load voltage has been dropped and distorted from 3.3 s. The load decrease does not affect grid voltages. However, the impact is visible on load voltages, where the load decrease has a significant influence when utilizing the traditional PQ. The correction is substantially quicker and more efficient when using the proposed PQ.

THD for grid voltage and load voltage with traditional and proposed PQ technique with a 50% reduction in load is shown in Figure 21C. It can be observed for grid voltage, THDs with traditional and proposed methods are displaying the same THDs for before, during, and after compensation. For load voltage, the THD with traditional PQ measure at before, during, and after compensation is 1.7%, 18.23%, and 4.89% respectively. With the proposed PQ method for all the conditions of before, during, and after compensation. The measured THD values are 1.14%, 4.23%, and 1.41% under before, during, and after compensation respectively. These THD values suggest the effectiveness of the proposed PQ method.

The comparison of the amplitude of grid voltage and load voltage before and during with traditional and Proposed PQ methods for 50% load change is shown in Figure 21D. It can be observed that the grid voltage measured with traditional and Proposed PQ methods are identical with 1 pu for all scenarios of before, during, and after compensation. With the proposed PQ the load voltage had demonstrated an acceptable voltage quality of nearly 1 pu when compared to the traditional PQ control.

Figure 22A explains the experimental results of 50% load change using the traditional PQ control strategy. Under these conditions, the load voltage has more distortion from the instant of 50% load change from 0.05 s. Whereas, the grid voltage remains constant at 1 pu. The experimental results of the grid, load, and compensating voltage for the proposed

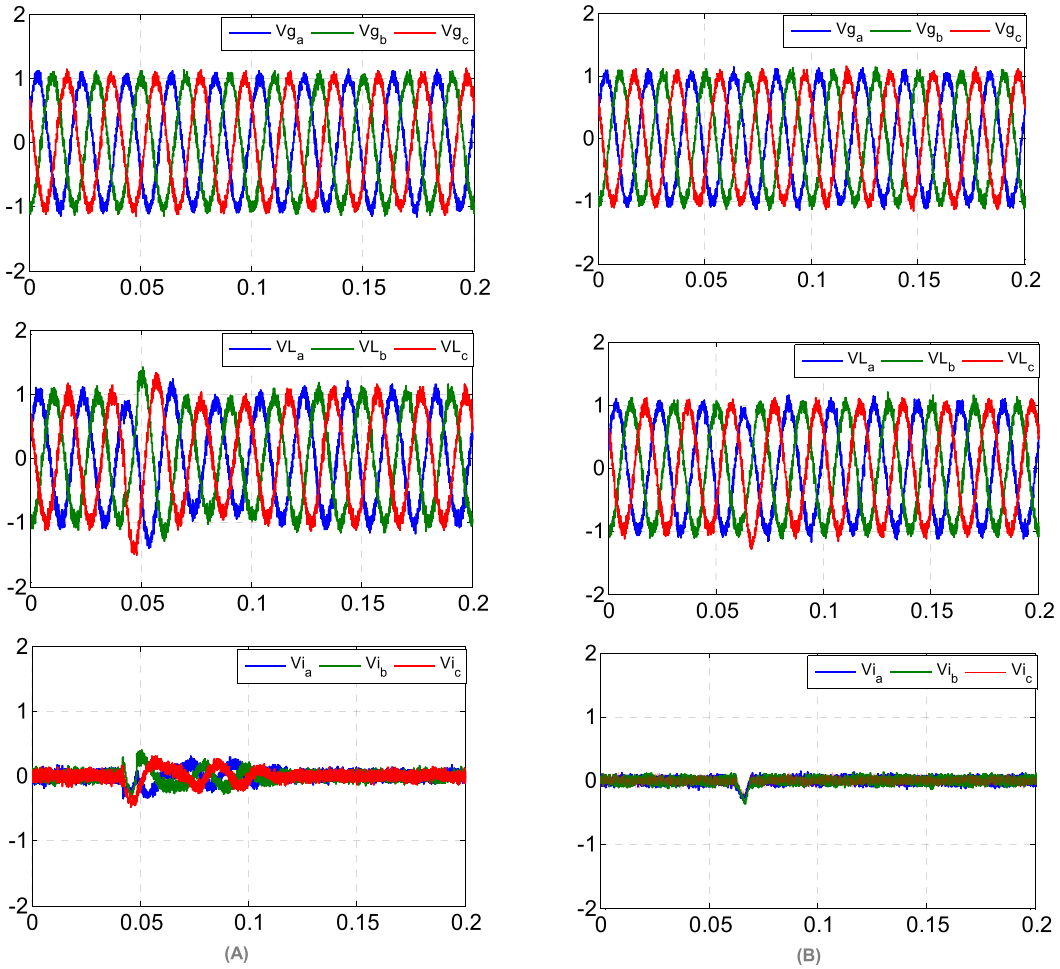

FIGURE 22. Experimental results of grid voltages, load voltage and DVR voltages (a) traditional PQ (b) modified PQ under 50% load change.

PQ technique are shown in Figure 22B. It can be observed under the 50% load change load voltage has been well compensated with very few distortions as depicted in Figure 22C. From Figure 22D, the load voltage profile has improved completely under this proposed PQ control for 50% load change.

The per-unit load voltage and frequency for the improved and traditional PQ techniques are shown in Figure 23. It is observed that the load variation had largely affected the load voltage with a change in voltage from 3.3 s to 3.45 s. The maximum observed change is 0.3 pu at 3.325 s and got settled to the nominal voltage at 3.475 s. Whereas, with the proposed PQ the change in load voltage is observed from 3.3 s to 3.325 s with a maximum load voltage change of 0.75 pu at 3.305 s. The load voltage settled down to the nominal value very fast at 3.325 s.

For load frequency with the traditional approach, the change in load frequency is observed from 3.3 s to 3.45 s with a maximum change of 0.25 Hz at 3.34 s. Whereas, with the modified PQ approach the change in frequency is from 3.3 s to 3.36 s with a maximum change of 0.05 Hz at 3.34 s. When comparing the traditional and proposed PQ control approach, it can be observed that the load voltage and frequency fluctuations are larger with the traditional PQ control approach.

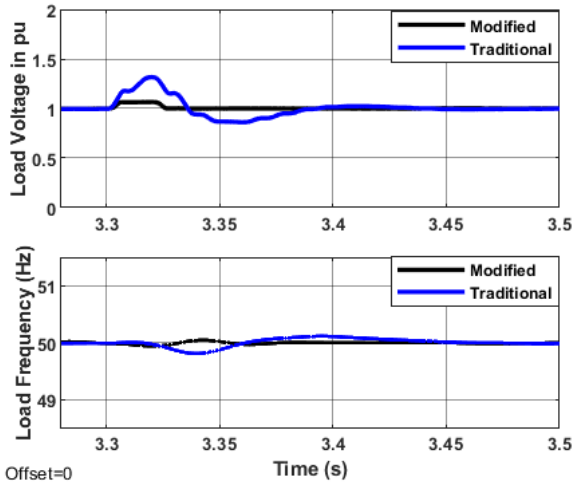

FIGURE 23. [Upper] PU load voltage, [lower] load frequency under 50% load change.

VI. CONCLUSION

This paper delivered a method for compensating voltage disturbances while using the DVR. The proposed approach improves the quality of load voltages by protecting them against grid voltage abnormalities. The proposed DVR control approach is based on a modified version of PQ theory that employs a detection method for the positive and negative sequence components. The detection technique is carried out in the time domain. The efficiency of the proposed approach is assessed using extensive simulations in MATLAB/Simulink and experiments under several special disturbance scenarios: severe unbalanced sag and swell, load change, and voltage harmonics. The proposed method has shown capability in improving the voltage quality as well as the voltage profile. The results have emphasized the applicability of the proposed DVR compensation method. To sum up, the following advantages summarize the performance of the proposed system:

- Less computational effort.
- Faster response.
- Balanced load voltages under severe unbalanced voltage sag and swell.
- Effective harmonic cancelation.
- Less transient oscillation in the fundamental frequency.

REFERENCES

[1] S. A. Mohammed, A. G. Cerrada, A. M. M. Abdel-Rahim, and B. Hasanin, "Dynamic voltage restorer (DVR) system for compensation of voltage sags, state-of-the-art review," *Int. J. Comput. Eng. Res.*, vol. 3, no. 1, pp. 2250–3005, 2013.

[2] A. I. Pathan, S. S. Vanamane, and R. H. Chile, "Different control techniques of dynamic voltage restorer for power quality problems," in *Proc. 1st Int. Conf. Autom., Control, Energy Syst. (ACES)*, Feb. 2014, pp. 1–6.

[3] N. Hosseinzadeh, A. Aziz, A. Mahmud, A. Gargoom, and M. Rabbani, "Voltage stability of power systems with renewable-energy inverter-based generators: A review," *Electronics*, vol. 10, no. 2, pp. 1–27, Jan. 2021, doi: 10.3390/electronics10020115.

[4] Y. Jani, S. Savaliya, V. Solanki, and A. Mahavidyalaya, "A review on dynamic voltage restorer (DVR) to improve power quality," *Int. J. Eng. Sci. Res. Technol.*, vol. 3, no. 2, pp. 1–5, 2014.

[5] S. Jothibasu and M. K. Mishra, "A control scheme for storageless DVR based on characterization of voltage sags," *IEEE Trans. Power Del.*, vol. 29, no. 5, pp. 2261–2269, Oct. 2014, doi: 10.1109/TPWRD.2014.2316598.

[6] F. K. de Araújo Lima, J. M. Guerrero, F. L. Tofoli, C. G. C. Branco, and J. L. Dantas, "Fast and accurate voltage sag detection algorithm," *Int. J. Electr. Power Energy Syst.*, vol. 135, Feb. 2022, Art. no. 107516, doi: 10.1016/j.ijepes.2021.107516.

[7] S. F. Al-Gahtani, A. B. Barnawi, H. Z. Azazi, S. M. Irshad, J. K. Bhutto, H. M. Majahar, and E. Z. M. Salem, "A new technique implemented in synchronous reference frame for DVR control under severe sag and swell conditions," *IEEE Access*, vol. 10, pp. 25565–25579, 2022, doi: 10.1109/ACCESS.2022.3151919.

[8] S. Suraya and K. S. R. Anjaneyulu, "SRF controlled DVR for compensation of balanced and unbalanced voltage disturbances," *Int. J. Electr. Eng. Technol.*, vol. 7, no. 3, pp. 73–92, 2016.

[9] E. A. Al-Ammar, A. Ul-Haq, A. Iqbal, M. Jalal, and A. Anjum, "SRF based versatile control technique for DVR to mitigate voltage sag problem in distribution system," *Ain Shams Eng. J.*, vol. 11, no. 1, pp. 99–108, Mar. 2020, doi: 10.1016/j.asej.2019.09.001.

[10] S. Nawaz, N. Jhajharia, and T. Manglani, "Reduction of distribution losses by combined effect of feeder reconfiguration and optimal capacitor placement," *Int. J. Recent Res. Rev.*, vol. 2, pp. 30–38, Jun. 2012.

[11] R. O. Bawazir and N. S. Cetin, "Comprehensive overview of optimizing PV-DG allocation in power system and solar energy resource potential assessments," *Energy Rep.*, vol. 6, pp. 173–208, Nov. 2020, doi: 10.1016/j.egyr.2019.12.010.

[12] M. Farhadi-Kangarlu, E. Babaei, and F. Blaabjerg, "A comprehensive review of dynamic voltage restorers," *Int. J. Electr. Power Energy Syst.*, vol. 92, pp. 136–155, Nov. 2017, doi: 10.1016/j.ijepes.2017.04.013.

[13] C. Zhan, "Dynamic voltage restorer with battery energy storage for voltage dip mitigation," in *Proc. 8th Int. Conf. Power Electron. Variable Speed Drives*, 2000, pp. 360–365, doi: 10.1049/cp:20000273.

[14] G. S. Chawda, A. G. Shaik, O. P. Mahela, S. Padmanaban, and J. B. Holm-Nielsen, "Comprehensive review of distributed facts control algorithms for power quality enhancement in utility grid with renewable energy penetration," *IEEE Access*, vol. 8, pp. 107614–107634, 2020, doi: 10.1109/ACCESS.2020.3000931.

[15] T. Bhattacharjee, M. Jamil, and A. Jana, "Design of SPWM based three phase inverter model," in *Proc. Technol. Smart-City Energy Secur. Power (ICSESP)*, Mar. 2018, pp. 1–6, doi: 10.1109/ICSESP.2018.8376696.

[16] N. Abas, S. Dilshad, A. Khalid, M. S. Saleem, and N. Khan, "Power quality improvement using dynamic voltage restorer," *IEEE Access*, vol. 8, pp. 164325–164339, 2020, doi: 10.1109/ACCESS.2020.3022477.

[17] J. Afonso, C. Couto, and J. Martins, "Active filters with control based on the P-Q theory," *IEEE Ind. Electron. Soc. Newslett.*, vol. 47, no. 3, pp. 5–10, Sep. 2000. [Online]. Available: http://hdl.handle.net/1822/1921

[18] A. Eltamaly, Y. Sayed, A.-H. Ahmed, and A. A. Elghaffar, "Mitigation voltage sag using DVR with power distribution networks for enhancing the power system quality," *Int. J. Electr. Eng. Appl. Sci.*, vol. 1, no. October, pp. 2600–7495, 2018.

[19] J. Han, X. Kong, P. Li, Z. Zhang, and X. Yin, "A novel low voltage ride through strategy for cascaded power electronic transformer," *Protection Control Modern Power Syst.*, vol. 4, no. 1, pp. 1–12, Dec. 2019, doi: 10.1186/s41601-019-0137-1.

[20] A. H. Soomro, A. S. Larik, M. A. Mahar, A. A. Sahito, A. M. Soomro, and G. S. Kaloi, "Dynamic voltage restorer—A comprehensive review," *Energy Rep.*, vol. 7, pp. 6786–6805, Nov. 2021, doi: 10.1016/j.egyr.2021.09.004.

[21] A. Mortezaei, C. Lute, M. G. Simoes, F. P. Marafao, and A. Boglia, "PQ, DQ and CPT control methods for shunt active compensators—A comparative study," in *Proc. IEEE Energy Convers. Congr. Exposit. (ECCE)*, Sep. 2014, pp. 2994–3001, doi: 10.1109/ECCE.2014.6953807.

[22] M. K. Mishra and V. N. Lal, "An improved methodology for reactive power management in grid integrated solar PV system with maximum power point condition," *Sol. Energy*, vol. 199, pp. 230–245, Mar. 2020, doi: 10.1016/j.solener.2020.02.001.

[23] M. I. Hossain, I. Rahaman, M. N. Rahman, and R. C. Sarker, "Voltage SAG compensation in distribution system using dynamic voltage restorer," in *Proc. 2nd Int. Conf. Adv. Inf. Commun. Technol. (ICAICT)*, Nov. 2020, pp. 28–29.

[24] B. Bae, J. Jeong, J. Lee, and B. Hen, "Novel sag detection method for line-interactive dynamic voltage restorer," *IEEE Trans. Power Del.*, vol. 25, no. 2, pp. 1210–1211, Apr. 2010, doi: 10.1109/TPWRD.2009.2037520.

[25] R. Nasrollahi, H. F. Farahani, M. Asadi, and M. Farhadi-Kangarlu, "Sliding mode control of a dynamic voltage restorer based on PWM AC chopper in three-phase three-wire systems," *Int. J. Electr. Power Energy Syst.*, vol. 134, Jan. 2022, Art. no. 107480, doi: 10.1016/j.ijepes.2021.107480.

[26] A. Karthikeyan, D. G. A. Krishna, A. Tejaswini, A. S. Panda, and R. L. Prasanna, "A comparative study of PI and PDF controllers for DVR under distorted grid conditions," in *Proc. 20th Nat. Power Syst. Conf. (NPSC)*, Dec. 2018, pp. 1–6, doi: 10.1109/NPSC.2018.8771444.

[27] S. N. Abdulazeez, D. Atilla, and C. Aydin, "Design of adaptive controller for regulating the voltage by a dynamic voltage restorer DVR," in *Proc. 2nd Int. Conf. Electr., Commun., Comput., Power Control Eng. (ICECCPCE)*, Feb. 2019, pp. 13–14.

[28] G. A. de Almeida Carlos, C. B. Jacobina, J. P. R. A. Mello, and E. C. D. Santos, "Cascaded open-end winding transformer based DVR," *IEEE Trans. Ind. Appl.*, vol. 54, no. 2, pp. 1490–1501, Mar. 2018, doi: 10.1109/TIA.2017.2768531.

[29] E. H. Watanabe, H. Akagi, and M. Aredes, "Instantaneous P-Q power theory for compensating nonsinusoidal systems," in *Proc. Int. School Nonsinusoidal Currents Compensation*, Jun. 2008, pp. 1–10, doi: 10.1109/ISNCC.2008.4627480.
[30] P. Li, L. Xie, J. Han, S. Pang, and P. Li, "New decentralized control scheme for a dynamic voltage restorer based on the elliptical trajectory compensation," *IEEE Trans. Ind. Electron.*, vol. 64, no. 8, pp. 6484–6495, Apr. 2010, doi: 10.1109/TPWRD.2009.2037520.
[31] S. P. C. Rao, "Enhancement of fast loop controlling mechanism for capacitor-supported dynamic voltage restorer (DVR) using modulation technique," *Int. J. Eng. Res. Appl.* , vol. 3, no. 2, pp. 1474–1491, 2013.
[32] D. S. Pillai and N. Rajasekar, "A comprehensive review on protection challenges and fault diagnosis in PV systems," *Renew. Sustain. Energy Rev.*, vol. 91, pp. 18–40, Aug. 2018, doi: 10.1016/j.rser.2018.03.082.
[33] S. P. Mishra, B. Biswal, J. P. Roselyn, and D. Devaraj, "Simulation and analysis of DVR for mitigating voltage sags and swells," *Proc. Eng.*, vol. 64, pp. 341–350, Jan. 2013, doi: 10.1016/j.proeng.2013.09.106.
[34] S. A. Singh and S. S. Williamson, "Comprehensive review of PV/EV/grid integration power electronic converter topologies for DC charging applications," in *Proc. IEEE Transp. Electrific. Conf. Expo (ITEC)*, Jun. 2014, pp. 1–5, doi: 10.1109/itec.2014.6861766.
[35] I. S. F. Gomes, Y. Perez, and E. Suomalainen, "Coupling small batteries and PV generation: A review," *Renew. Sustain. Energy Rev.*, vol. 126, Jul. 2020, Art. no. 109835, doi: 10.1016/j.rser.2020.109835.
[36] M. I. Hossain, I. Rahaman, M. N. Rahman, M. F. Hasan, M. M. Hasan, and R. C. Sarker, "Voltage sag compensation in distribution system using dynamic voltage restorer," in *Proc. 2nd Int. Conf. Adv. Inf. Commun. Technol. (ICAICT)*, Nov. 2020, pp. 492–497, doi: 10.1109/ICAICT51780.2020.9333502.
[37] M. Pradhan and M. K. Mishra, "Dual $P-Q$ theory based energy-optimized dynamic voltage restorer for power quality improvement in a distribution system," *IEEE Trans. Ind. Electron.*, vol. 66, no. 4, pp. 2946–2955, Apr. 2019, doi: 10.1109/TIE.2018.2850009.
[38] S. Suraya, S. M. Irshad, M. F. Azeem, S. F. Al-Gahtani, and M. H. Mahammad, "Multiple voltage disturbance compensation in distribution systems using DVR," *Eng., Technol. Appl. Sci. Res.*, vol. 10, no. 3, pp. 5732–5741, Jun. 2020, doi: 10.48084/etasr.3485.
[39] P. S. Babu and N. Kamaraj, "Performance analysis of DVR using ANN controller for voltage quality enhancement," *Appl. Mech. Mater.*, vol. 573, pp. 356–361, Jun. 2014, doi: 10.4028/www.scientific.net/AMM.573.356.
[40] S. N. Abdulazeez, D. Atilla, and C. Aydin, "Design of adaptive controller for regulating the voltage by a dynamic voltage restorer DVR," in *Proc. 2nd Int. Conf. Electr., Commun., Comput., Power Control Eng. (ICECCPCE)*, Feb. 2019, pp. 165–170, doi: 10.1109/ICECCPCE46549.2019.203767.
[41] R. S. Al Abri, E. F. El-Saadany, and Y. M. Atwa, "Optimal placement and sizing method to improve the voltage stability margin in a distribution system using distributed generation," *IEEE Trans. Power Syst.*, vol. 28, no. 1, pp. 326–334, Feb. 2013, doi: 10.1109/TPWRS.2012.2200049.
[42] V. K. Remya, P. Parthiban, V. Ansal, and A. Nandakumar, "Single-phase DVR with semi-Z-source inverter for power distribution network," *Arabian J. Sci. Eng.*, vol. 43, no. 6, pp. 3135–3149, Jun. 2018, doi: 10.1007/s13369-017-2841-3.
[43] H. H. Alhelou, M. Hamedani-Golshan, T. Njenda, and P. Siano, "A survey on power system blackout and cascading events: Research motivations and challenges," *Energies*, vol. 12, no. 4, p. 682, Feb. 2019, doi: 10.3390/en12040682.
[44] S. Jain, "Fuzzy controller based DVR to mitigate power quality and reduce the harmonics distortion of sensitive load," *Int. J. Adv. Res. Elect., Electron. Instrum. Eng.*, vol. 1, no. 5, pp. 351–361, Nov. 2012.
[45] N. G. El Sayed, G. El-Saady, E.-N.-A. Ibrahim, and M. A. Mohamed, "Dynamic voltage restorer for enhancing distribution systems power quality," in *Proc. 7th Int. Japan-Africa Conf. Electron., Commun., Comput., (JAC-ECC)*, Dec. 2019, pp. 210–215, doi: 10.1109/JAC-ECC48896.2019.9051252.
[46] D. Petreus, S. Daraban, I. Ciocan, T. Patarau, and C. Morel, "Single-stage low cost grid connected inverter in photovoltaic energy applications," in *Proc. 15th Int. Power Electron. Motion Control Conf. (EPE/PEMC)*, Sep. 2012, pp. 1–6, doi: 10.1109/EPEPEMC.2012.6397351.
[47] A. Pakharia and M. Gupta, "Dynamic voltage restorer for compensation of voltage SAG and swell?: A literature review," *Int. J. Adv. Eng. Technol.*, vol. 4, no. 1, pp. 347–355, 2012.
[48] G. Devadasu, S. Muthubalaji, S. Srinivasan, and A. Gunde, "An experimental approach of DVR for relieving voltage dip and voltage swells," *Mater. Today, Proc.*, Feb. 2021, doi: 10.1016/j.matpr.2021.01.056.
[49] A. H. Mollah, P. G. K. Panda, and P. P. KSaha, "Single phase grid-connected inverter for photovoltaic system with maximum power point tracking," *Int. J. Adv. Res. Electr., Electron. Instrum. Eng.*, vol. 4, no. 2, pp. 648–655, Feb. 2015, doi: 10.15662/ijareeie.2015.0402021.
[50] M. P. F. Asna and M. V. M. Kumar, "Dstatcom for distribution system having high PV penetration," in *Proc. Int. Conf. Power Electron. Appl. Technol. Present Energy Scenario (PETPES)*, Aug. 2019, pp. 1–5.
[51] A. Farooqi, M. M. Othman, M. A. M. Radzi, I. Musirin, S. Z. M. Noor, and I. Z. Abidin, "Dynamic voltage restorer (DVR) enhancement in power quality mitigation with an adverse impact of unsymmetrical faults," *Energy Rep.*, vol. 8, pp. 871–882, Apr. 2022, doi: 10.1016/j.egyr.2021.11.147.
[52] P. Thankachen and D. A. Thomas, "Hysteresis controller based fault current interruption using DVR," in *Proc. Annu. Int. Conf. Emerg. Res. Areas: Magn., Mach. Drives (AICERA/iCMMD)*, Jul. 2014, pp. 1–4.